CHALMERS
UNIVERSITY OF TECHNOLOGY

Digital Twin: Potentials for Radio Environment Simulations and Analysis

Master's thesis in Communication Engineering

CHITRA SURESH HEBBAR

DEPARTMENT OF ELECTRICAL ENGINEERING

CHALMERS UNIVERSITY OF TECHNOLOGY
Gothenburg, Sweden 2024
www.chalmers.se

Master's thesis 2024

Digital Twin: Potentials for Radio Environment Simulations and Analysis

CHITRA SURESH HEBBAR

CHALMERS
UNIVERSITY OF TECHNOLOGY

Department of Electrical Engineering
Division of Communication Engineering
Chalmers University of Technology
Gothenburg, Sweden 2024

Digital Twin: Potentials for Radio Environment Simulations and Analysis
CHITRA SURESH HEBBAR

Supervisors: Per Skarin, Ericsson; Charitha Madapatha, Chalmers
Examiner: Tommy Svensson, Department of Electrical Engineering, Chalmers

Master's Thesis 2024
Department of Electrical Engineering
Division of Communication Engineering
Chalmers University of Technology
SE-412 96 Gothenburg

Typeset in LaTeX
Gothenburg, Sweden 2024

Digital twin: Potentials for Radio Environment Simulations and Analysis
CHITRA SURESH HEBBAR
Department of Electrical Engineering
Chalmers University of Technology

Abstract

The rapid evolution of wireless technology, especially, in the context of 5G and beyond, requires innovative solutions to meet the increasing demands of network scaling and complexity. The emergence of network digital twin has marked a significant leap forward in the management of network operations and maintenance. This thesis explores the concept of the network digital twin by performing 3D simulations using advanced tools, with a particular focus on 5G network scenarios. The study unfolds in three phases: initial simulations using the 3D simulator, integration of the tool with OpenAirInterface for core network functionality, and comparative analysis of the 3D simulator result with a standard theoretical model. Most of the work was focused on an indoor scenario, with the possibility to extend later for outdoor environments. The 3D simulator performed better in comparison to the theoretical model. The integration with OpenAirInterface worked successfully in terms of established connection and observed data traffic between base station and user equipment. There are potentials for further improvement by considering additional scenarios and scalability.

Keywords: Digital Twin, 3D Simulation, Radio access network, OpenAirInterface.

Acknowledgements

I express my gratitude to my supervisors, Per Skarin and Charitha Madapatha, for their unwavering guidance throughout this thesis. Their continuous support, patience and vast knowledge helped me navigate all stages of this thesis. I am grateful to my examiner Tommy Svensson for his valuable guidance throughout. I gratefully acknowledge the team at Ericsson for giving me the opportunity to work on this thesis and all those who generously shared their expertise and helped me with various technical aspects. Finally, I express my gratitude to my family for their immense support.

Chitra Suresh Hebbar, Gothenburg, June 2024

List of Acronyms

Below is the list of acronyms that have been used throughout this thesis listed in order of occurrence:

DT	Digital twin
NDT	Network digital twin
RAN	Radio access network
RIS	Reconfigurable intelligence surface
SNR	Signal-to-noise ratio
SLS	System level simulator
LLS	Link level simulator
E2ES	End-to-end simulator
3D	Three Dimensional
BS	Base station
UE	User equipment
OAI	OpenAirInterface
SDR	Software defined radio
3GPP	3rd Generation Partnership Project
SA	Standalone
NSA	Non-Standalone
OAI-RAN	OpenAirInterface (OAI) Radio access network
OAI-CN	OAI Core network
EPC	Evolved packet core
CN	Core network
eNB	Evolved Node B
gNB	Next Generation Node B
AMF	Access and Mobility Management Function
SMF	Session Management Function
UPF	User Plane Function
NRF	Network Repository Function
NF	Network Function
5GCN	5G core network
PDU	Protocol data unit
SPGW	Serving packet data network gateway
SPGWU	Serving packet data network gateway user plane
SSRSRP	Synchronization signal based reference signal received power

RSRP	Reference signal received power
RF	Radio frequency
RTT	Round trip time
RRC	Radio resource control
DRB	Data radio bearer
MCS	Modulation and coding scheme
BLER	Block error rate

Contents

List of Figures

List of Tables

1
Introduction

Wireless technology is advancing rapidly towards new generations, significantly faster compared to just a few years ago [1]. This advancement has created a need for faster growth in network infrastructure to meet the scaling demands across networks. To improve performance levels, network operations and maintenance are becoming increasingly complex due to the high degree of sophisticated services provided by these networks. Consequently, the challenge of innovating network technologies and operations is complicated by potential infrastructure disruption and high field trial costs. Furthermore, the future generations of network technologies are anticipated to be even more complex and flexible. To effectively manage these challenges, many simulation tools are explored at various stages of the communication system.
The latest simulation technology involves immersive visualization and detailed real-world modeling called a digital twin (DT). Enhanced capability with this technology could enable better product performance, short time to market, and simplify the introduction of new functionalities in the radio access network [2]. To sustain a high pace of product innovation together with optimal system performance, new generation of simulation technologies is devised continuously. They provide a convenient approach towards design, testing, and validation of network models.
The main motive to introduce simulations in radio networks is to evaluate and analyze the performance before deployment. They help identify potential problems, the need for optimization, and possible design improvements. Simulation enables the testing of a variety of scenarios that may not be feasible in real-world testing. By simulating a network model, different scenarios and configurations can be explored without any risk.
Another important aspect of 5G and beyond (6G) is that it is much more than a generational upgrade in bandwidth, as it involves the transformation of the access network to make it more like a cloud platform. Technology trends such as software-defined networking and open source software will lead to an innovative and flexible RAN. The new requirements that 5G anticipates include higher traffic volumes, many more concurrent devices with different service requirements, better quality of user experience and better affordability by reducing costs.

1.1 Background

Simulation in the context of radio networks is a technique to build and evaluate a system, process and concept. Simulation makes it possible to build mathematical as well as computer based models in virtual space allowing simplified visualization of

some complex scenarios, in turn allowing for the determination of effective solutions. In general, simulation plays a critical role in radio network design and optimization by providing a cost-effective and scalable approach to test and refine the network throughout its life cycle.
Over the years, the use of simulation in radio networks has evolved to include the concept of DTs. Unlike simulation, which provides a model of the system, DT is a virtual representation of the entire process in real world. The DT takes simulation to the next level by incorporating real-time data from the physical world into the model [3]. The concept of DT was first introduced in 2002 by Dr. Michael Grieves, a comprehensive overview of its history can be found in [4], [5]. As a cross-platform game engine, this concept has swiftly risen to prominence in the video game industry and is frequently employed in developing over 60% of mobile games, augmented reality (AR), and virtual reality (VR) content that is presently marketed. This DT concept is widely used in various industries as it facilitates seamless design, testing, and analysis [6].
A network digital twin (NDT) is a digital representation of the real-world network, mapping original network assets, objects, and other entities in a virtual space as illustrated in Figure 1.1. This enables the assessment of numerous functionalities and the evaluation of network performance without physically deploying it in the real world. DT bridges the gap between simple channel emulator tests and expensive as well as hard to control over the air (OTA) tests in real deployments. Despite being at an early stage of development, NDT could be a potential tool for understanding the possible outcomes of performance and operational management of a network.

Figure 1.1: Example of a real-world city environment, modeled in a DT simulator [7]

1.2 Objective

The objective of this thesis is to develop a simulation on a DT model of the radio environment that replicates the real-world radio environment. The study involves identifying relevant parameters that contribute to the accuracy of the model and analyzing their impact in the replicated environment. The main emphasis is on the replication and evaluation of the radio access network (RAN) component of the

wireless network. The simulations are performed using an internal tool developed by Ericsson, aiming to advance knowledge in this direction. The task involves the integration of this tool with an open source software for cellular networks. The research will provide insights into the potential of simulation and DT models to accurately replicate the radio environment and aid in the optimization of network design.

1.3 Limitations

Due to complexity of the topic and given time constraints, there are few limitations in this study. The scope of this project is to develop and evaluate simulation environments that replicate real-world RANs, using existing channel models and scenarios. However, this work does not include the design of channel modeling, as the focus is on the evaluation of the simulated environment. Additionally, existing three dimensional (3D) model of scenarios are utilized for simulations rather than developing new scenarios from scratch, due to the time-intensive nature of 3D asset creation. While future work could potentially expand the modeling and scenario complexity, the current project emphasizes developing RAN simulations within the constraints of leveraging established channel models and pre-existing 3D assets.

1.4 Sustainability and Ethical aspects

DT can provide significant sustainability benefits by optimizing wireless infrastructure utilization and reducing resource wastage [8]. Traditional practices like drive testing require extensive truck rolls and fuel consumption to characterize RAN performance, identification of problems in the network and to validate the effects of applied changes in the network. Furthermore, there will be unnecessary costs of deployment in cases where reproducing an issue would be necessary to identify root causes and evaluate solutions. Digital twins minimize this environmental impact by enabling accurate virtual modeling [9]. Additionally, a site DT helps in the safety of personnel by reducing the tower climbs. However, ethical considerations around data privacy must also be considered. Collecting detailed data on network architectures and usage profiles raises concerns if not managed properly. Anonymization, transparency, and consent are critical in implementing digital twin solutions ethically [10]. For RAN modeling specifically, care must be taken to abstract sensitive subscriber information while still achieving sufficient fidelity. With thoughtful implementation, DTs present a sustainability opportunity while safeguarding ethical priorities.

1.5 Thesis Outline

This report is structured into 6 chapters, each contributing to a comprehensive understanding of the research. Following the Introduction, Chapter 2 focuses on DT concepts and OpenAirInterface (OAI), providing a detailed exploration of the the-

oretical underpinnings and state-of-the-art. Chapter 3 outlines the methodological approach undertaken in the study, shedding light on the steps and tools employed. In Chapter 4, the emphasis shifts towards the discussion of the research findings, with a particular focus on performance in conjunction with the broader research context. Chapter 5 and 6 serve as the culmination of this report, offering a conclusive summary of the main insights derived from the study and possible future work.

2

Theory and System Model

2.1 Concept of Digital Twin in Radio Network

DT has several definitions in different contexts evolved over the time. Originally coined by Dr. Michael Grieves [11], it is defined as a virtual model used to simulate, emulate, mirror or twin a physical world entity with an object or process. In [12], DT is emphasised to be a technology more than a simple simulation model. A DT consists of three components: a physical world, a virtual space or DT model, and the connection between them through data and information exchange as depicted in Figure 2.1. As shown, the physical world is a product or process in the physical environment. The virtual space or DT model represents the twin of the physical world in a virtual environment. Here, the two environments are linked by the exchange of information and data from the virtual environment to the physical environment and data exchange in the other direction. The link enables cooperation between the two environments and the flow of information. The information derived from

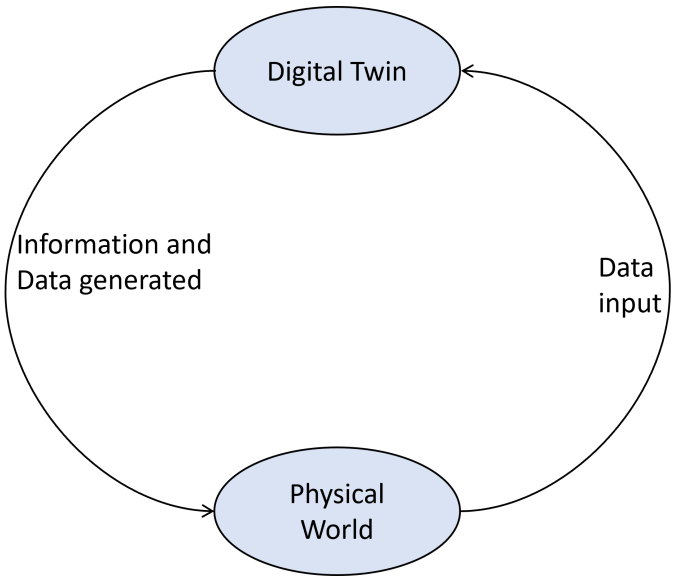

Figure 2.1: Simplified Model of DT concept

the DT provides details about the product specifications and the process, while the data generated indicates the data that would have been collected while they had a particular operation or process taken place in the physical world. The data derived from the actual product or process in the physical world is fed into the DT and

used to make predictions and control decisions. Additionally, with advancements in modeling, the input could include optimization algorithms and machine learning methods. The key concept of DT is to develop a model that replicates complex real-world systems, thus easing the complexity of operations.
The fundamental concepts of DT and simulation differ but are complementary. Though simulations are not new, digital twins are still relatively emerging. As previously defined, a digital twin obtains data from the physical world via interconnected sensors, machinery or other cloud-based applications. The scope of a simulator is often limited to a specific process, but not always. Conversely, a DT will often encompass broader processes or multiple simulations and tend to remain connected to the real-world. A combination of simulation and DT could create immensely powerful outcomes [12].
Generally, there are prerequisites to develop a DT model. The essential requirements are a model of a physical environment in the form of a DT and the behavior of that environment. Here, DT has to reflect the physical environment in a more accurate way including all the assets and their functionalities. The more data collected and fed to the DT, the better the information generated. Using the information from DT, the model can be continuously improved to reach better understanding and thereby to find optimal solutions. It can predict the behavior of how the physical products would perform over time with the real time data collected.
A Network Digital Twin (NDT) is a virtual replica of the physical network in the real world. It is possible to replicate an entire network or part of it, which includes real-world objects, systems, and processes. These models are then used to tune and adjust the network parameters to study the effect in the physical world that was being replicated.
NDT can be a model of an individual physical network component like radio access network (RAN), core network or transport network. It can also be a combination of network entities like twin of a cell site/near edge/far edge/cloud, or a twin of an entire end-to-end physical network. The two pillars of DT are physically accurate model and its demonstration with simulation, visualization and control. One of the requirements of modelling include accuracy of the model, which is particularly important considering the next generation of cellular networks (6G) using THz with ultra-wide signal bandwidth, integrated radar, lidar sensing, with large antennas and incorporated reconfigurable intelligence surface (RIS).

2.2 State-of-the-art

As DT is a relatively new area in wireless communications, literature on its design and evaluation is limited. However, the industry utilizes several simulators, which are primarily categorized into three types ,i.e., Link level, system level and an end-to-end simulator. In wireless network simulation, a link level simulator (LLS) focuses on modelling communication between individual nodes, providing granular insights into the performance of specific links within the network. A system level simulator (SLS), on the other hand, operates at a higher level of abstraction and examines the overall behavior of the network, considering multiple links, base stations, and user equipment. It evaluates aspects such as interference, network capacity, and

handover strategies. An end-to-end simulator (E2ES) covers the entire communication path from source to destination, taking into account the complete network infrastructure and protocol stack. It evaluates overall system performance, including factors such as data throughput, latency and overall network efficiency, providing a comprehensive view of the network's capabilities.
Below describes some of the most widely adopted simulators in the industry. NS3 [13] stands out as one of the most extensively used simulators for wireless networks. It is an open-source simulator that provides a broad range of features, supporting different network protocols and technologies. The learning curve for NS3 is steep, and sufficient programming skills are required to use it effectively. Conversely, Amarisoft [14] is another popular simulator that focuses on simulating 4G and 5G networks, delivering user-friendly and accessible interface to support a range of network configurations. Amarisoft is renowned for its significant performance and scalability, which enables the simulation of large-scale networks. Nevertheless, since it is a commercial simulator, users may incur licensing fees. Other wireless network simulators that are commonly used include OMNeT++ [15], MATLAB [16], and OPNET [17]. OMNeT++ is an open-source simulator that supports various network protocols and technologies. The software provides a graphical user interface and permits discrete event and continuous simulation. As it is modular and extensible, it can be complex to set up simulations and the learning curve may be steep. Additionally, OMNeT++ could be limited in scalability and performance for large scale simulations. MATLAB is a commonly used simulation and modelling tool that provides a wide range of functions and toolboxes for network simulation, but it is proprietary and requires a licence, which limits open use and research. On the other hand, OPNET is a open source simulator with extensive features that support several network protocols and technologies. Nevertheless, it is limited to customisation and scalability, compared to its counterparts.

2.2.1 OpenAirInterface (OAI)

OAI [18] is an open-source software platform that focuses on the simulation and emulation of 4G and 5G networks. Its flexible and customizable framework allows researchers and developers to conveniently experiment with network protocols and technologies. OAI fully complies with the standards defined by the 3rd Generation Partnership Project (3GPP)[1]. By aligning with 3GPP standards, OAI ensures compatibility and interoperability with commercial network equipment, whilst facilitating the development of innovative solutions within established industry standards.
As an open source project, it allows for increased transparency, collaboration and community involvement to promote innovation and knowledge sharing. Furthermore, OAI provides support for both simulation and emulation, offering additional benefits. Simulation enables the evaluation of network performance under controlled conditions, while emulation allows the testing of real-world scenarios using actual hardware. This flexibility enables the validation of findings in both virtual and real environments. Alternative implementations of 5G new radio exist in the software

[1]3GPP is a global collaboration of telecommunications standards organizations that defines specifications for mobile communication systems, including 4G and 5G networks [19].

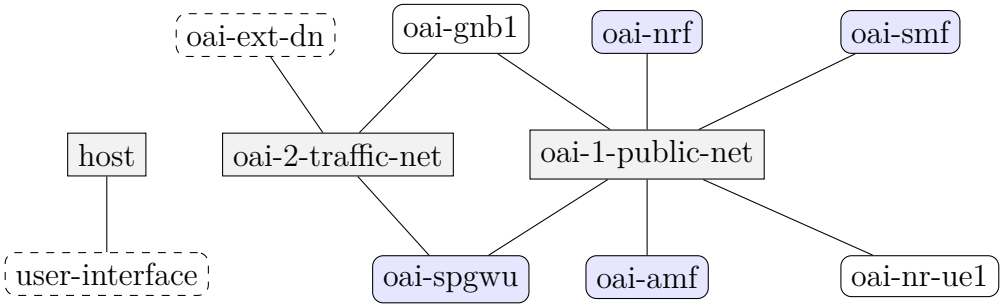

Figure 2.2: Docker containers and network setup. Gray boxes are communication networks and rounded boxes are containers, with blue showing the 5G core.

defined radio (SDR) field, but the OAI project stands out as the only completely open source endeavour with a public license. Therefore, it is easy to integrate with the tool, which will be discussed in Chapter 3.
OAI offers a 4G as well as standalone (SA) and non-Standalone (NSA) 5G stack implementation consisting of mainly two components: OAI Radio access network (OAI-RAN) and OAI Core network (OAI-CN). OAI-RAN supports the implementation of 4G LTE and 5G Radio Access Network including NodeB and User Equipment (UE). On the other hand, OAI-CN covers 4G LTE evolved packet core (EPC) and 5G core network (CN). This complete end-to-end solution for 5G SA mode includes [20],

- **NR UE:** An SDR based implementation of 5G UE supporting 5G SA mode control and user plane,
- **gNB:** An SDR based next generation node B (gNB) implementation with 5G SA mode features (and NSA support),
- **5GCN:** 5G core network implementation with access and mobility management function (AMF), session management function (SMF), user plane function (UPF) and network repository function (NRF) through docker based containerized deployment.

The deployed docker infrastructure is illustrated in Figure 2.2. Here, we see the AMF (oai-amf) that handles access and mobility, the SMF that manages the user session, i.e., where an IP protocol data unit (PDU) session is established - the NRF (oai-nrf) that provides service discovery, and a user plane serving packet data network gateway (SPGW) (oai-spgwu) connected to both OAI networks. There is also a MySQL container not illustrated in the figure. This setup, AMF, SMF, UPF (SPGWU), NRF, MYSQL, provides the minimum 5G core functional testing of OAI.
The oai-gnb1 and oai-nr-ue1 are containers that provide the gNB and a user communication device (the user equipment (UE)). This UE will be attached to one of the users in the simulation environment. There are also two dashed boxes. One is the user interface created in-house. The other is the oai-ext-dn which is an optional component used to send traffic to the UE. The AMF receives all connection and session information from the UE and is responsible for connection and mobility management tasks. The SMF then takes care of managing the session. The

SPGW is responsible for routing and sending packets. Additionally, it takes care of packet inspection, QoS management and external PDU session for data network (DN) interconnection. The role of the NRF is to provide control of virtual network functions (VNF) and the services offered by these functions.

2.3 Theoretical System Model

This section provides a detailed description of the theoretical approach used to compare the 3D simulation results of the tool from a theoretical perspective. The system model is based on the indoor hotspot model described in 3GPP TR 38.901 [21]. This indoor scenario aims to cover different indoor deployments, including office spaces and shopping malls. The indoor open room scenario used for tool simulation in Section 4.1.1 closely resembles the indoor open office scenario mentioned by 3GPP. The theoretical model compares the results of this scenario. It is worth noting that measurements collected from the tool only covers the downlink connection.

2.3.1 Channel Model

The received power at the user node is given by

$$P_{\mathrm{r}} = P_{\mathrm{tx}} \cdot G_{\mathrm{t}} \cdot G_{\mathrm{r}} \cdot \gamma \cdot L_{\mathrm{material}} \cdot h. \tag{2.1}$$

Here, P_{tx} represents the transmit power, G_{t} and G_{r} are the transmitter and receiver antenna gains respectively. γ denotes the propagation path loss between the transmit and receive nodes. The material loss in the scenario is indicated by L_{material}, and h denotes independent small scale fading, modelled as a normalized Rayleigh random variable. The path loss in dB for the indoor model, as outlined by 3GPP [21], is expressed by

$$\begin{aligned} \gamma_{\mathrm{LoS}} &= 32.4 \ + 17.3 \log_{10}(d_{3D}) + 20 \log_{10}(f_c), \\ \gamma\prime_{\mathrm{NLoS}} &= 38.3 \log_{10}(d_{\mathrm{3D}}) \ + 17.3 \ + 24.9 \log_{10}(f_c), \\ \gamma_{\mathrm{NLoS}} &= \max(\gamma_{\mathrm{LoS}}, \ \gamma\prime_{\mathrm{NLoS}}). \end{aligned} \tag{2.2}$$

Here, the 3D distance d_{3D} in indoor environment is considered over the range 1 m to 150 m and γ_{LoS} and γ_{NLoS} indicate the path loss concerning line of sight and non-line of sight paths. Each individual link has a distinct path loss, dependent on the line of sight probability that is defined by

$$\mathrm{Pr}_{LoS} = \begin{cases} 1 & d \leqslant 5\mathrm{m} \\ \exp\left(-\frac{d-5}{70.8}\right) & 5\mathrm{m} < d \leqslant 49\mathrm{m} \\ \exp\left(-\frac{\mathrm{d}-49}{211.7}\right) \cdot 0.54 & 49\mathrm{m} < d. \end{cases} \tag{2.3}$$

Here, as shown in (2.3) the model assumes that each link experiences independent blocking, such that the blocking experienced by one link does not affect the blocking experienced by other links. This generalises the analysis and provides an approximation when more complex blockage models are not necessary. Independent blockage model is chosen due to the limited correlation between the blockers in our system. In

addition, we consider the material loss that accounts for potential material losses in the scenario. Since this is an indoor scenario, other external losses such as outdoor to indoor penetration are neglected. Moreover, the channel model is applicable in the frequency range of 0.5 to 100 GHz as mentioned in [21].
An illustration of the indoor scenario from the tool, is discussed subsequently in Figure 2.3, and acts as the basis for the theoretical model. It is assumed that the placement of BS and UE is stationary in this case. The UE is initially positioned at the center, and can move to different locations, while the BS is fixed on the wall. To make the comparison simple and convenient, four points have been chosen where the position of the UE is noted and the corresponding distance between the positions of the UE and the BS is obtained. The marked points are considered UE positions, selected based on the observed rapid variation in the tool results. In addition, the interference from other UEs is neglected since we consider only one UE in this scenario. Thus, the comparison of the results is based on this scenario.

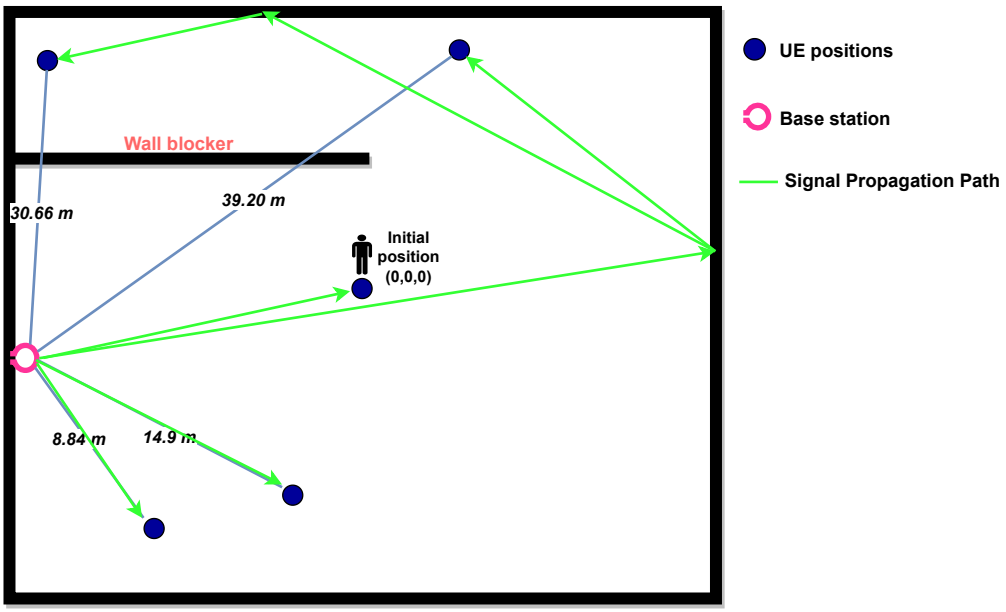

Figure 2.3: Illustration of Indoor scenario for theoretical model

2.3.2 Performance Metrics

There are a number of performance metrics which can be considered in the evaluation of the effectiveness of a digital twin tool. Based on the available parameters extracted directly from the simulation logs, the received power and throughput derived from it would be considered in this work as a metric for comparison. Accordingly, the received power in the downlink is calculated using Equation (2.1). The signal-to-noise ratio (SNR) ratio is calculated as below

$$SNR = \frac{P_r}{P_{\text{Noise}}}. \tag{2.4}$$

Here, P_{Noise} is the noise power. The throughput representing the maximum achievable rate in ideal conditions is calculated as below

$$T = BW \cdot \log_2(1 + SNR), \tag{2.5}$$

where BW represents the bandwidth. To ensure statistical robustness and account for the inherent variability introduced by randomization, the throughput obtained over 1000 simulations is averaged to compare with the throughput obtained from 3D simulator output. By this way, we try to understand the synergies of our methods.

3
Methodology

This chapter describes the methods used in the thesis. The workflow comprises three stages: 3D simulation and integration of OAI with the 3D simulator, followed by a comparison with theoretical model. Initially, the tool stage will be outlined, and the findings will be recorded. Then, the integration with OAI is detailed, and the outcomes are presented.

3.1 Overview of the 3D simulator

The digital twin tool designed by Ericsson has three sub-components that together contribute towards a functioning DT model as shown in Figure 3.1. These interrelated blocks enable the creation, exploration and evaluation of virtualized radio environments, contributing to enhanced understanding and optimization of wireless networks. Each component is briefly explained featuring their contributions in the design of DT model.

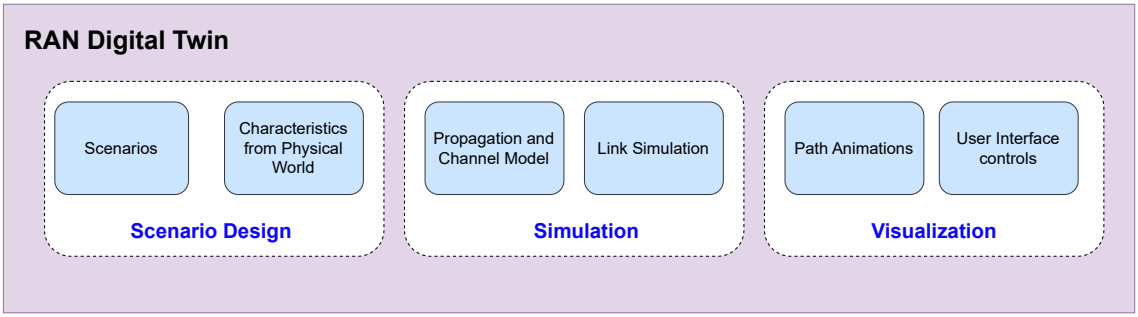

Figure 3.1: Block Diagram of components of RAN Digital Twin

3.1.1 Scenario Design

A 3D model of the scenario is created, and all network assets are inserted. Considering an example of an outdoor scenario, physical assets such as base stations (BSs), UEs and buildings, roads, and vehicles, as well as other possible assets are added. Here, models created using graphical software tools such as Blender [22] are imported. By designing a scenario, the size and complexity of the model can be controlled. However, in this work, existing scenarios were used to ensure feasibility, and to suit the constrained timeline. Further insights can be gained by working on designing new scenarios in the future.

3.1.2 Simulation

In the simulation phase, the computation of the channel model and propagation paths is conducted through an internal software component, which has already been seamlessly integrated. For the link simulation, an exploration will be undertaken to assess the potential integration of an open-source software, OAI, with this tool. This integration will facilitate an in-depth analysis of the traffic between UE and BS, consequently enhancing the validation process in a more precise manner. Currently, on top of the baseband of the tool, the CN and RAN from OAI are integrated. The OAI implements an open source 3GPP stack: the radio access network (evolved Node B (eNB), gNB) and 4G, 5G UE, as well as the core network (EPC and 5G CN). OAI supports three deployment platforms [23], out of which deployment of network functions (NFs) in docker containers will be used in this context. This specific component is the primary focus of this project, which is discussed in detail in subsequent sections.

3.1.3 Visualization

Visualization is essential for the ability to virtually explore the interesting features of a DT model throughout its life cycle. It can be visualised in real time as the network is being tuned for optimum performance. Features that are not visible in real life can be seen here. In line with propagation paths and user interactions, a rendering and collaborative design from the NVIDIA omniverse [2], is integrated to provide a complete visualization of access networks. This involves the development of in-house network models with unprecedented accuracy in real-world measurements. As future networks are expected to become increasingly complex, models will require comprehensive visualization support to be meaningful. NVIDIA Omniverse Create, utilizing the Unity game engine, integrates an innovative ray tracing engine with interactive interface for manipulating and exploring complex scenes. This allows for experimentation with product placement choices and the analysis of their real-time impact.

3.2 Simulation Setup

The simulations were carried out with a main focus on the indoor use cases. However, a limited simulations were also performed on outdoor use cases. This section summarizes the simulation setup, options considered and parameters. For simulations, a part of DT model setup was deployed on a cloud platform as shown in Figure 3.2 and integrated with OAI. In the figure, OAI components refer to the docker containers deployed in this thesis mentioned in Figure 2.2 and its relevant section. Only the 5G system from OAI will be the focus of this thesis, and it will be connected with the path calculations and channel from the scenarios in the tool.

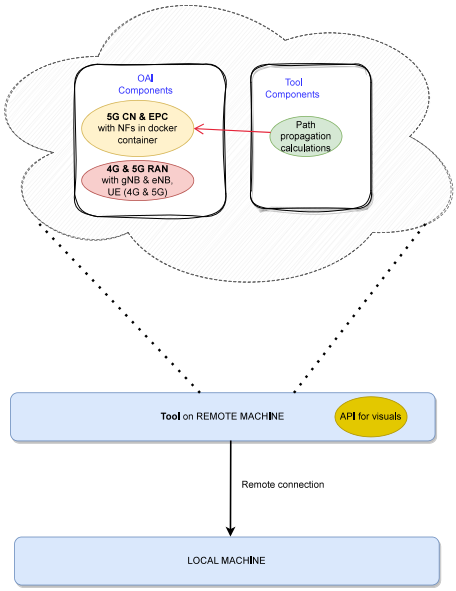

Figure 3.2: RAN DT implementation setup of Tool with OAI

3.2.1 Scenarios

There are two main simulation scenarios to consider, i.e., indoor and outdoor. For the indoor scenario, simulations are performed with up to 10 UEs moving at varying distances from the BS, which remains stationary throughout. Parameters were modified within each case and the results are recorded. The following scenarios were setup in the tool and experiments performed with varying parameters:

1. Indoor Basic Room
    - 1 UE and 1 BS
    - 10 UEs and 1 BS
    - 1 UE and 2 BSs
2. Outdoor
    - 1 UE and 5 BSs

3.2.2 Configuration

The tool is deployed on a remote machine and is accessed via a secure remote connection. The visualization engine is run locally, while the dependent applications

and function modules, together with the path propagation calculation, are in the cloud platform.

3.2.3 Parameters considered

From the pre-defined network parameters in the tool, those considered for simulation are listed in Table 3.1.

Table 3.1: Input parameters considered from the tool

Parameter	Representation	Value
Carrier Frequency	f_c	4 GHz
Bandwidth	BW	20 MHz
Transmitter Power	P_{tx}	30 dBm
Antenna noise figure	NF	6 dB

3.2.4 Simulation Environment

The simulation environment used in this thesis is depicted in Figure 3.3, illustrating two scenarios. In both the cases, the radio is on the wall and the UE is represented by a red person in Figure 3.3a. This person represents the UE/user that can be moved around. The rays in the figure show simulation path connections between the BS and the UE. In Figure 3.3b, there are 10 UEs connected to one BS. The user in red will enable movement control, while the other UEs will follow designated paths. This environment currently allows the selection of the BS position, the initial UE position and the number of both BS and UE, as well as an option to toggle the transmission through the wall. The tool uses an in-house propagation model that considers diffraction, diffusion, scattering and material effects in the propagation calculations resulting in richer propagation paths with more bounces.

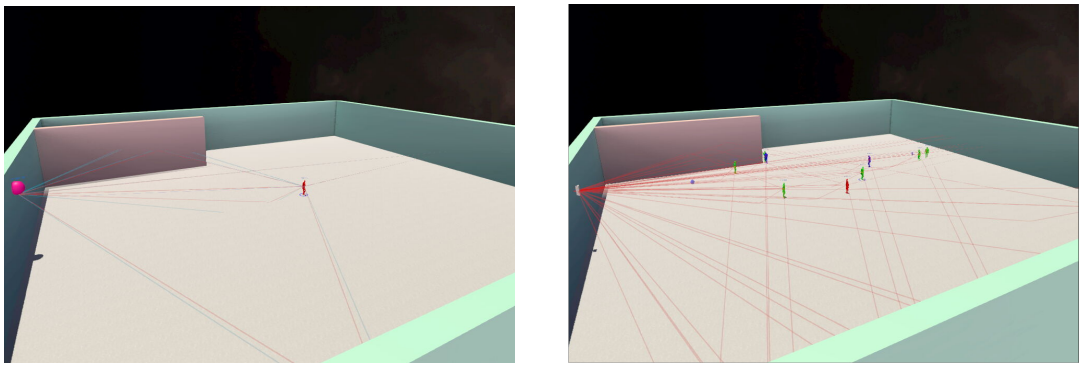

(a) 1 UE and 1 BS **(b)** 10 UEs and 1 BS

Figure 3.3: An instance of the simulation environment in the tool, illustrating two indoor scenarios.

3.3 Tool Integration with OAI

The OAI stack was integrated with the scenarios and parameters described in earlier setup, with the motive to investigate the potential of adding baseband and core network functionality to the 3D simulations. This section outlines the main steps taken and the observations made. For this purpose, OAI is integrated into the tool, which uses the core network components via virtual containers. This setup can easily be scaled as needed in the future. The Minimalist deployment is used, including MySQL (subscriber database), AMF, SMF, UPF, NRF only, thus building the 5G core network with the minimum number of network functions [23].

3.3.1 Setup

For successful deployment, OAI software is installed on a compatible Linux operating system that runs in the cloud. The individual OAI and tool components are deployed and accessed via separate containers in the cloud within a Docker environment. This setup involves installing the OAI software, the Docker engine and the 3D simulation components on a Linux machine followed by establishing a connection between the UE and the gNB using a scenario from the tool.

3.3.1.1 Prerequisites

The first step is to clone the OAI repositories:

```
git clone https://gitlab.eurecom.fr/oai/openairinterface5g.git
git clone https://gitlab.eurecom.fr/oai/cn5g/oai-cn5g-nrf
git clone https://gitlab.eurecom.fr/oai/cn5g/oai-cn5g-amf
git clone https://gitlab.eurecom.fr/oai/cn5g/oai-cn5g-smf
git clone https://github.com/OPENAIRINTERFACE/openair-spgwu-tiny
```

When integrating the OAI into the simulation environment, it is necessary to modify the configuration files so that they match the parameters, IP addresses, and other relevant factors in accordance with the requirements to ensure compatibility between the OAI and internal tool. After taking care of the dependencies, deploy the containers consisting gNB, UE, 3D tool and CN functions and ensure all the docker images are healthy as displayed below:

```
Network oai-1-public-net Created  0.1s
Network oai-2-traffic-net Created  0.1s
Container oai-nrf Started  1.0s
Container mysql  Healthy  3.5s
Container oai-nr-ue1 Started  3.8s
Container oai-amf Started  4.4s
Container oai-smf Started  4.9s
Container oai-spgwu Started  5.8s
Container oai-ext-dn Started  7.7s
Container oai-gnb1 Started  10.6s
```

In addition to the above container images of OAI components, the internal tools run in separate containers that are not displayed. It is possible for the UE container to communicate with the external network (oai-ext-dn) once all containers have been

started. This will be covered in the next section, where the ping and iperf3 utilities will be used to test the connection.

3.3.1.2 Traffic test with Ping and Iperf

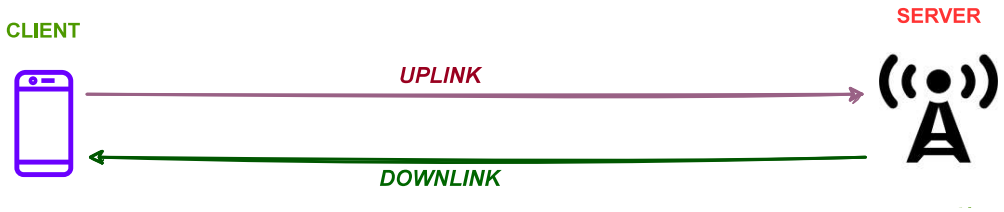

Figure 3.4: Server and client for Downlink and Uplink in Iperf3 test

The ping command is used to test connectivity between two devices in the network. It sends ICMP echo requests to a specified IP address or hostname and waits for a response (ICMP echo reply). In this scenario, the ping test serves as a basic connectivity check to verify that the network is functioning correctly between the nodes. It helps to ensure that the OAI deployment can successfully exchange data packets between the nodes in the network.
Iperf, also known as IP Performance, is an objective tool for testing and tuning network performance. With its ability to provide comprehensive measurement results for both wired and wireless networks, Iperf has become an essential utility for network professionals. It is a cross-platform application compatible with both Windows and Linux operating systems. It operates with client and server functionality and can generate data streams to measure the throughput between the two network nodes in one or both directions. The generated Iperf results include detailed, time-stamped data regarding the amount of data transferred and the measured throughput. A traffic test is performed here, between the UE and the oai-ext-dn. Any node can serve as iperf server/client as in Figure 3.4.

4

Results and Discussion

This chapter presents the simulation results and provides a brief discussion of these results.

4.1 3D simulations

This section presents the simulation results of the experiments performed using the propagation tool for the scenarios listed in Section 3.2.1.

4.1.1 Indoor Basic room

In the indoor setting, simulations were performed under identical conditions and parameters with varying number of BS and UE. The data collected from these simulation log was used to generate visual representations to study the tool's performance using Python scripts.

(a) 1 UE and 1 BS

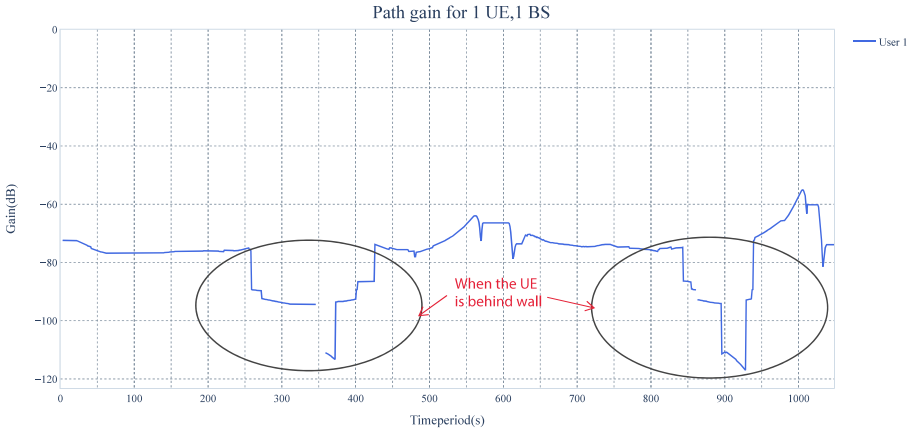

(a) Path gain

Figure 4.1: Measured values for the indoor scenario with 1 UE connected to 1 BS over the simulation duration.

In this scenario, an interactive UE and one BS were included. The simulation involved moving the UE from close proximity to the BS to far away, and behind an obstacle (in this case, a wall), with subsequent values of power and gain being observed.

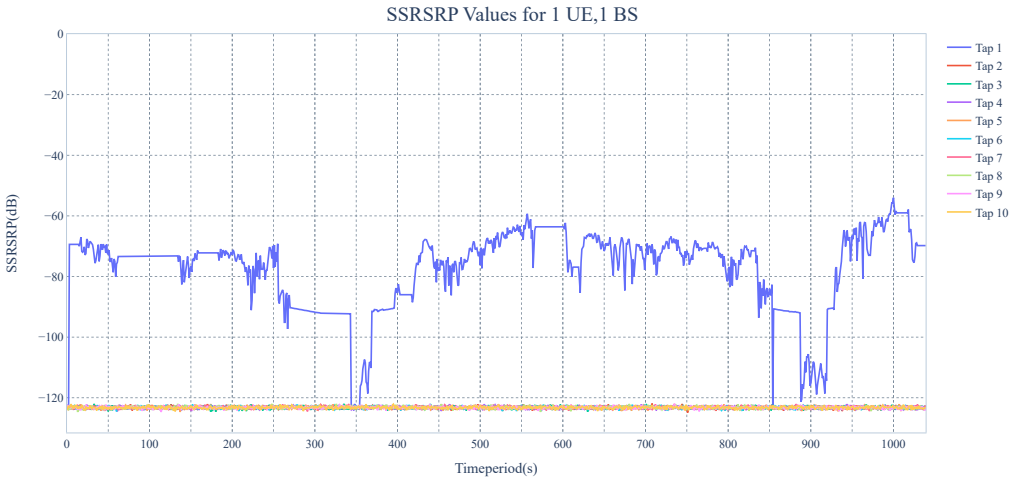

(b) SSRSRP

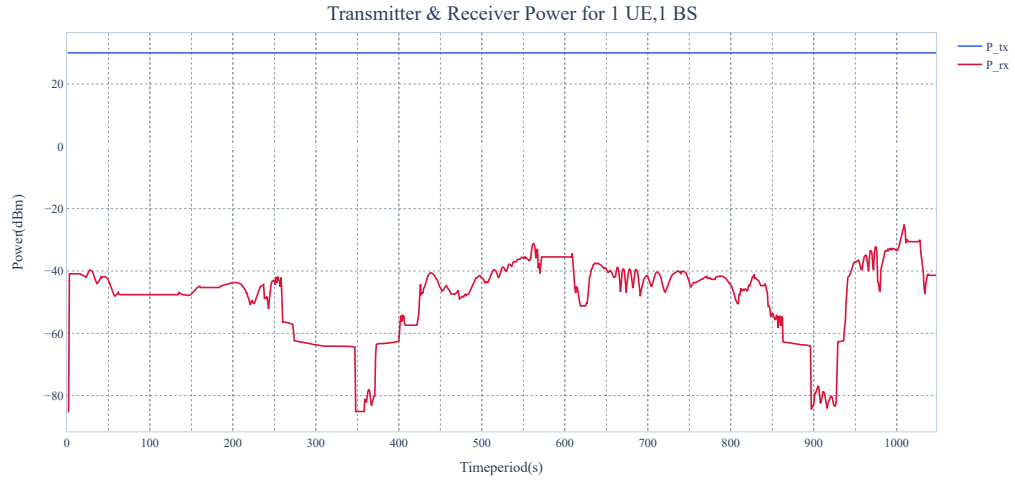

(c) Power

Figure 4.1: Measured values for the indoor scenario with 1 UE connected to 1 BS over the simulation duration.

Using the input parameters from 3.2.3, and a stationary BS, Figure 4.1 displays the measured values of path gain, synchronization signal based reference signal received power (SSRSRP) and received power for the UE when moving around the room in a simulation environment. The path gain precisely corresponds to the UE's movement in an expected manner. The marked area in Figure 4.1a displays the region when the UE moves behind the wall and lost the connection from BS. In this case, the

diffraction, diffusion and transmission through the wall were turned off. As there is only one base station in this scenario, the UE experiences a loss of connection when it moves out of coverage. However, it did reconnect upon returning to coverage, even after losing connection while moving behind an obstacle.

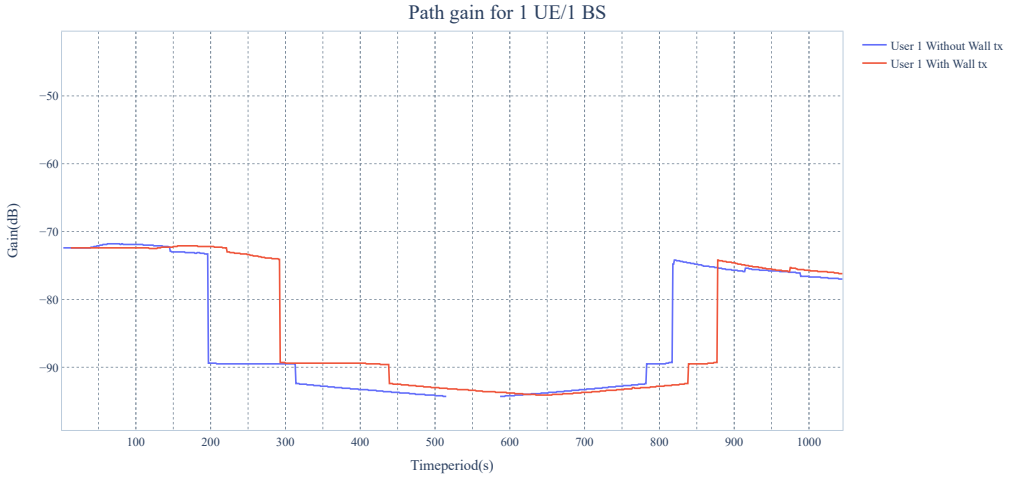

(a) Path gain

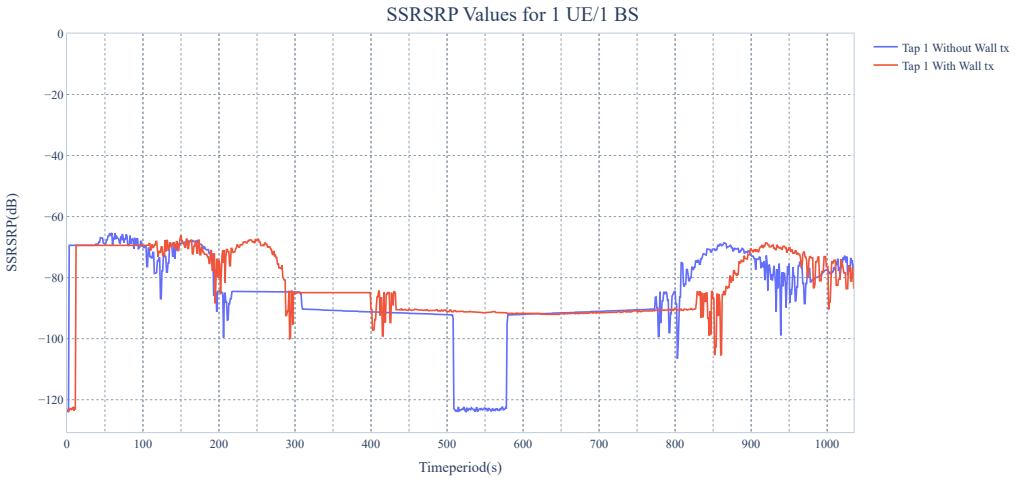

(b) SSRSRP

Figure 4.2: Graphs illustrating signal attenuation in scenarios where the UE is positioned behind a wall, comparing the conditions with and without wall transmission in 1 UE connected to 1 BS scenario.

In Figure 4.1b illustrates the SSRSRP which represents the average power of 5G cell synchronization signal in each resource element and is used to measure the receiving signal strength of the downlink synchronization signal. The reporting range is between -156 dBm to -31 dBm [24]. The SSRSRP falls below -100 dBm

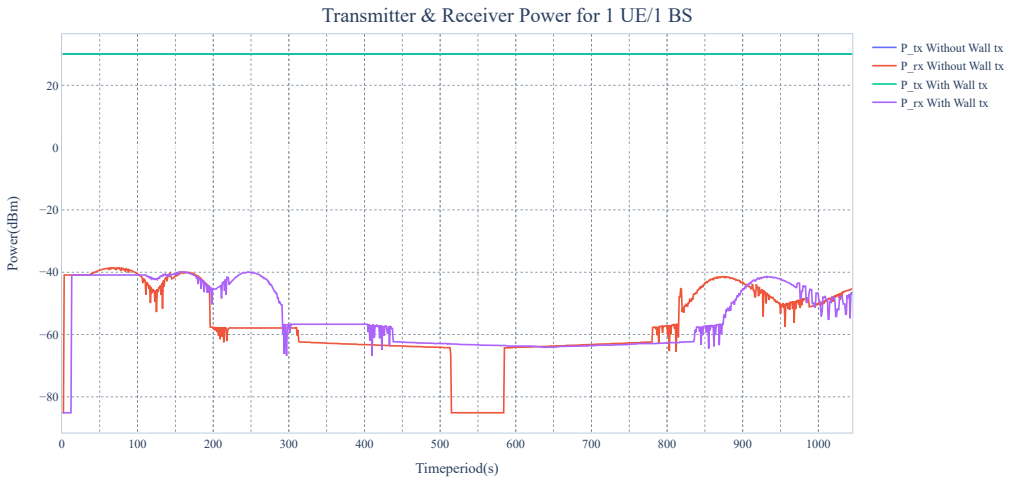

(c) Power

Figure 4.2: Graphs illustrating signal attenuation in scenarios where the UE is positioned behind a wall, comparing the conditions with and without wall transmission in 1 UE connected to 1 BS scenario.

when the UE loses connection. According to the recommended SSRSRP range [25], this value indicate cell edge condition. In contrast, when the UE is in close proximity to the BS, the SSRSRP values are above -80 dBm indicating good signal strength. The presence of obstacles between the BS and UE significantly alters the SSRSRP values, impacting signal coverage. It is apparent from the measurements that as the distance increases, the measured SSRSRP value tends to decrease due to the increase in propagation loss. Figure 4.1c shows the power received by the UE during the simulation period with a fixed transmit power. The value is associated with the UE's movement, and the tool logs downlink connection values.

Another case explored with the same setup, where a UE is moved behind the wall in the scene and the wall transmission, diffraction and diffusion features are turned on. The measurements of the corresponding parameters, as shown in Figure 4.2, depicts a clear signal drop and no connection to the BS when the UE is positioned behind an obstacle with no reflected transmissions. This aspect of high order propagation interactions provides channel richness and leads to realistic simulation measurements which can be visualized in real time. This scenario with 1 UE and 1 BS will be used with the OAI to verify the connections and data transfer in a subsequent section.

(b) 10 UEs and 1 BS

This scenario involves a stationary BS and ten mobile UEs, of which only one UE's position and movements is controlled. The path gain, SSRSRP and received power values for ten UEs connected to one BS in the same simulation environment as above are shown in Figure 4.3.

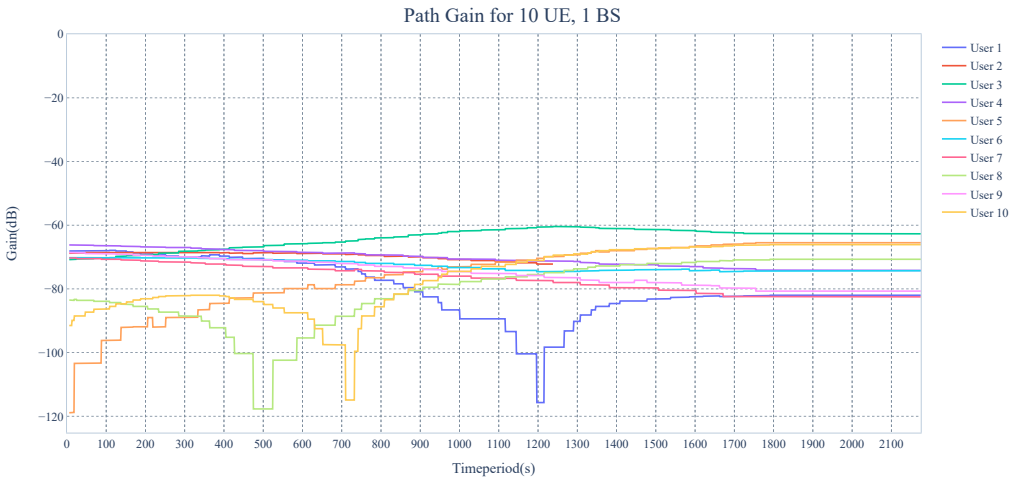

(a) Path gain

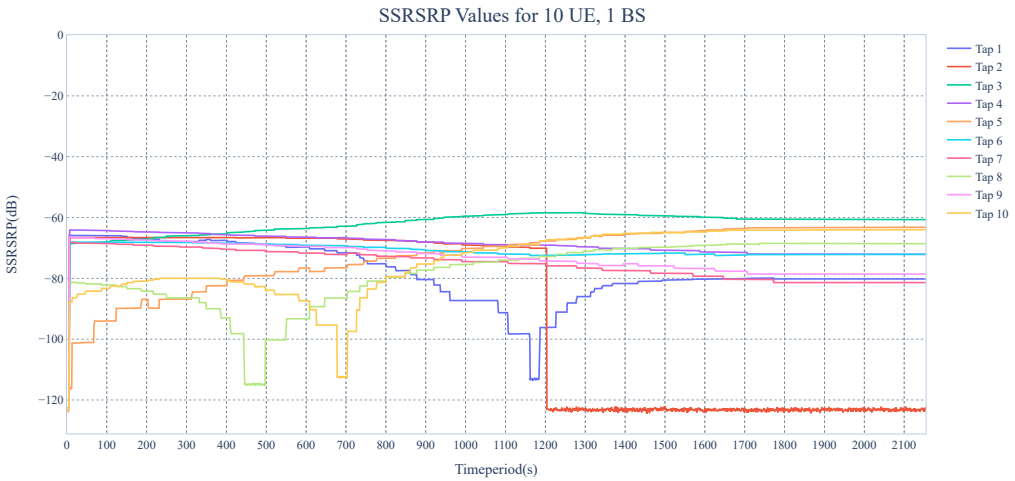

(b) SSRSRP

Figure 4.3: Measured values for the indoor scenario with 10 UEs connected to 1 BS over the simulation duration.

The received power from measurement logs represent the maximum power of all users, which ranges from -20 dBm and -40 dBm for the entire simulation period. For the gain and SSRSRP values, the addition of a further number of UEs makes it challenging to interpret insights from them. The User 2, having a specified path to follow and whose movement is not controlled, was apparently disconnected at 1230 seconds in the simulation duration and did not reconnect as observed in the path gain in Figure 4.3d. This is also reflected in the SSRSRP values. The reason for this behaviour, taking into account the observations made in the previous scenario, is probably that the user was obstructed by the wall and was unable to re-establish connection with the BS. Furthermore, with this scenario the potential for scalability

is seen, suggesting the possibility of expanding from a single user to a larger number of users, perhaps accommodating additional gNBs in the future.

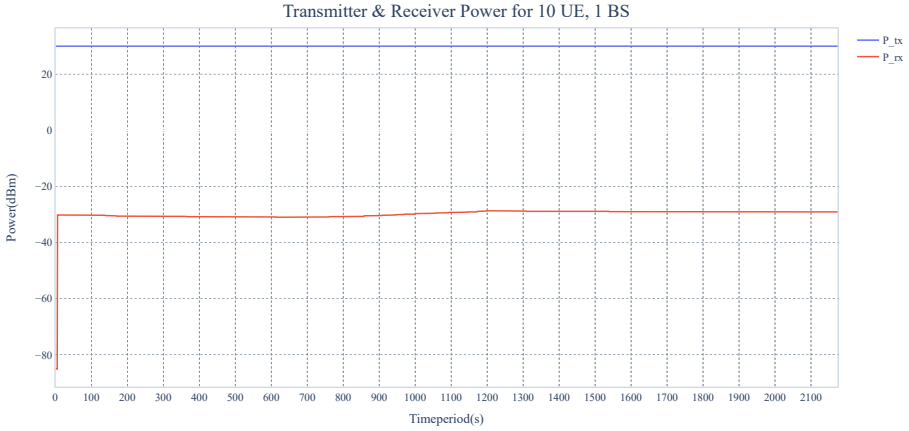

(c) Power

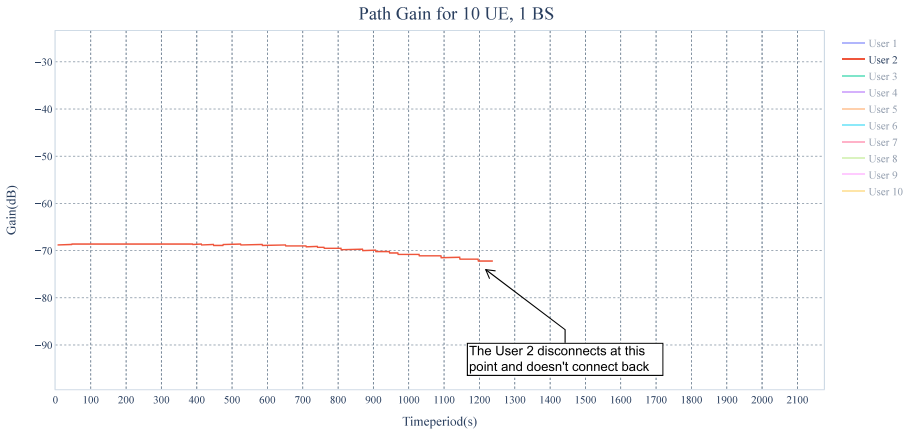

(d) Path gain for User 2

Figure 4.3: Measured values for the indoor scenario with 10 UEs connected to 1 BS over the simulation duration.

(c) 1 UE and 2 BS

In this scenario, the simulation environment is identical to the previous two scenarios. Here, two base stations are present and one interactive UE is moving around as illustrated in Figure 4.4a.

The shaded regions on the graphs presented in Figure 4.5 illustrate the base station to which the UE is connected during a specific time in the simulation duration.

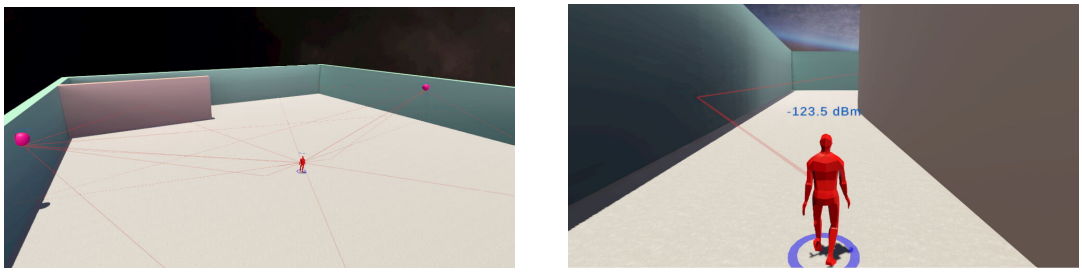

(a) Simulation Environment with 1 UE and 2 BS

(b) UE connected to a second BS when positioned behind an obstacle.

Figure 4.4: The simulation environment in the tool for a scenario with 1 UE 2 BS.

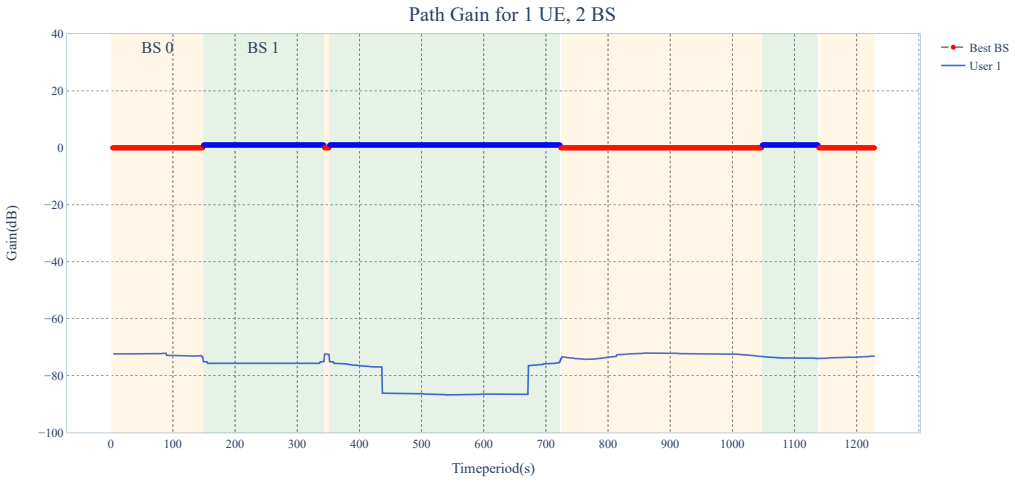

(a) Path gain

Figure 4.5: Measured values for the indoor scenario with 1 UE connected to 2 BSs over the simulation duration

The path gain and received power measurements in Figure 4.5 indicate that the UE remains connected to at least one of the BS at any given point, while moving around the corner.
However, there is still a drop in the SSRSRP values even though the UE is connected to the second BS, as can be seen in Figure 4.5b. The UE could establish a connection with the second BS in cases where it is obstructed and connectivity with the first BS is interrupted, as illustrated in Figure 4.4b. If this decrease in SSRSRP value is examined, it has the potential to significantly impact handover procedures.

4.1.2 Outdoor

1 UE and 5 BS

This scenario explores an outdoor environment in a densely populated urban area where the user is surrounded by buildings, trees and moving vehicles. The scenario

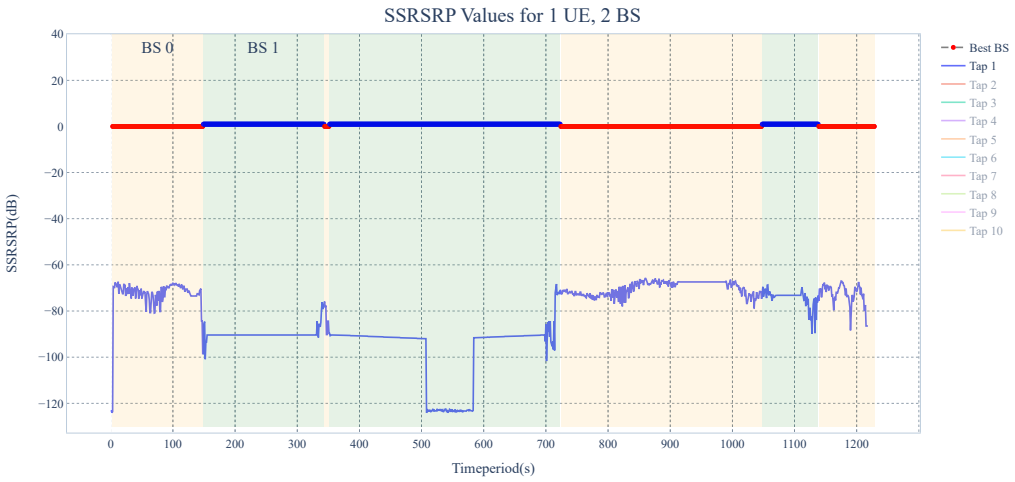

(b) SSRSRP

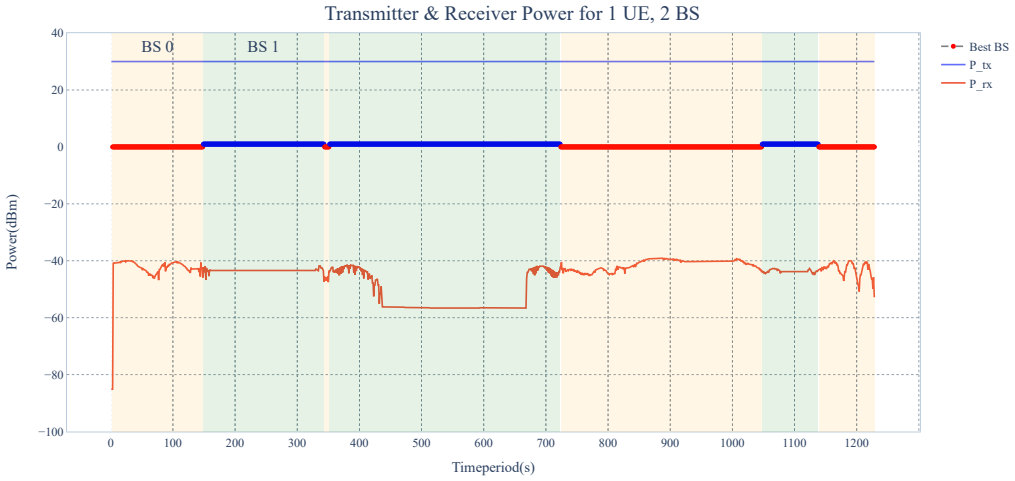

(c) Power

Figure 4.5: Measured values for the indoor scenario with 1 UE connected to 2 BSs over the simulation duration

consists of one UE and five BSs. The measurements of path gain, SSRSRP, and received power are recorded and plotted against the simulation duration as shown in Figure 4.6. The various colours in the best BS indicate the different BSs to which the UE is connected at a given point in simulation time. It has been noted that the various modules of the tool have a delay in loading, resulting in the measured values beginning at a timestamp of 128 seconds, particularly in an outdoor scenario. The notable variations observed in the measurements compared to the previous indoor scenario are mainly due to changes in the propagation conditions. This scenario includes different materials that introduce different propagation effects. The path gain depicted in Figure 4.6a experiences a notable decline, falling within the range

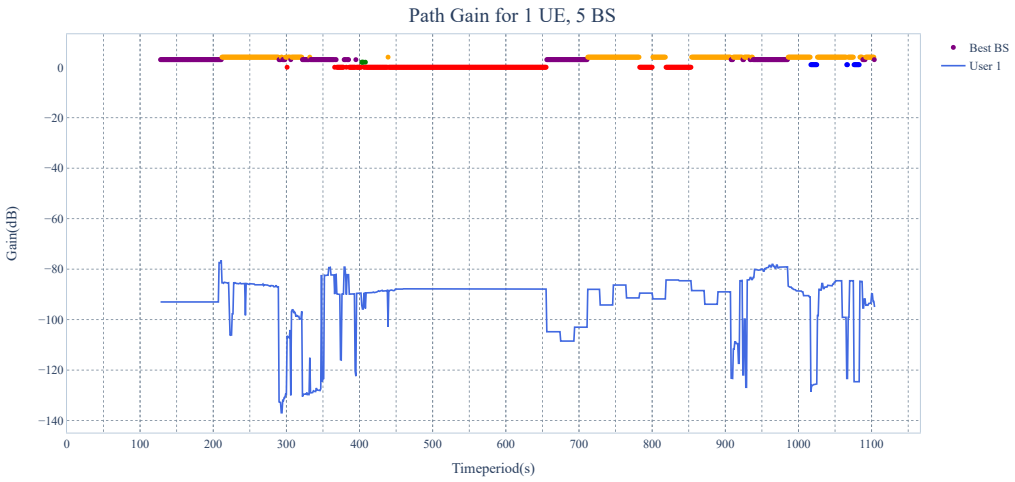

(a) Path gain

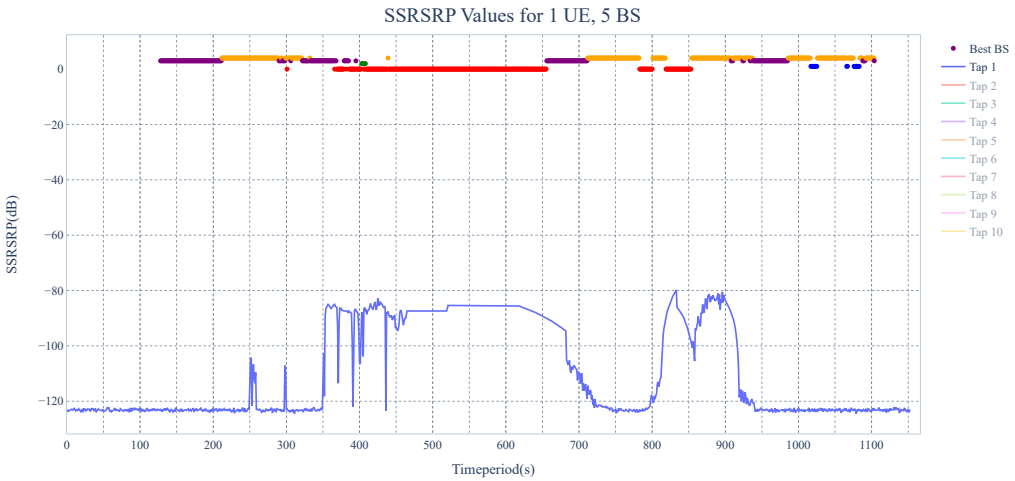

(b) SSRSRP

Figure 4.6: Measured values for the outdoor scenario with 1 UE connected to 5 BSs over the simulation duration

of -120 to -140 dB. This drop is primarily due to the incoherent sum of all paths in the link between the UE and the available BSs. This is also evident in the values of SSRSRP and received power. However, the enabling of reflection, diffraction, and diffusion ensured that the UE remained connected throughout the duration of the simulation without disconnections. In addition, the system attempts a handover as the UE moves between BSs, although the process may not be flawless, it seems to ensure uninterrupted connectivity, as can be seen in Figure 4.6, where different coloured markers indicate the BS to which the UE is connected at that time.

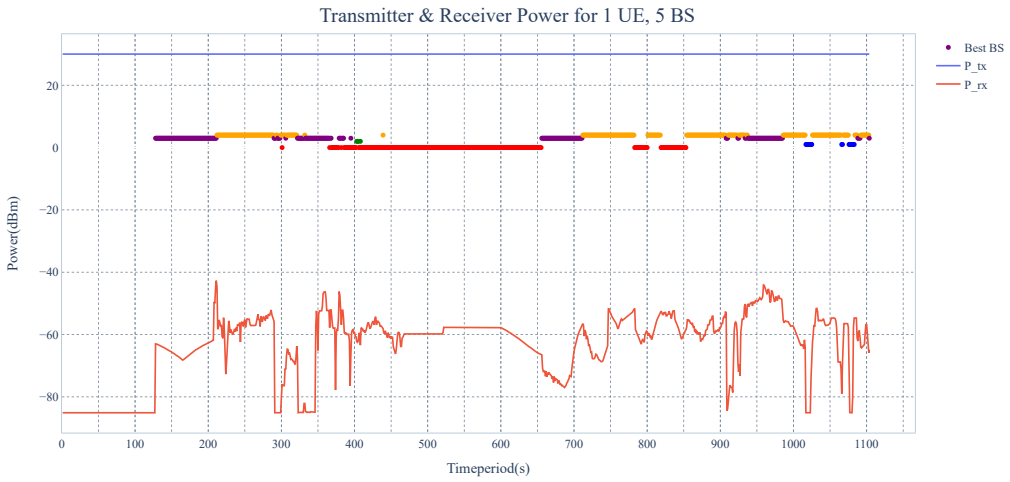

(c) Power

Figure 4.6: Measured values for the outdoor scenario with 1 UE connected to 5 BSs over the simulation duration

4.2 Simulations from OAI Integration

This section presents the simulation results of OAI using the scenario from the tool, followed by the results of the traffic test with ping and iperf.

4.2.1 OAI Network functions

The OAI minimalistic deployment utilizes the core NFs mentioned in Section 2.2.1, using oai-gnb in monolithic mode and oai-nr-ue in radio frequency (RF)-simulator mode. In the monolithic mode oai-gnb is implemented as a single network node. All the external components are connected to the CN through the AMF. As a first step after the deployment of containers, the oai-nrf container initializes, and the NRF starts functioning. Then each NFs such as AMF, SMF, and serving packet data network gateway user plane (SPGWU), register with the NRF. These registrations include information about their capabilities and locations. Then oai-gnb and oai-nr-ue1 initialize and register with the NRF. When these functions are up and running, it is verified by the log from oai-amf, which illustrates the initial connection status of the gNodeB and UE as in Figure 4.7. When the UE starts, it first completes the random access procedures with gNB and initiates registration and authentication with the CN. It also establishes a PDU session, after successfully registering with the CN. The traffic exchange for access procedure, registration and data transfer between UE and gNB is observed in the oai-gnb log. The data received by gNB are logged as ulsch_total_bytes_received as displayed in Figure 4.8. Whereas the data sent by gNB is logged as dlsch_total_bytes.

The oai-gnb logs record the data bytes exchanged and RSRP for each link (gNB-UE

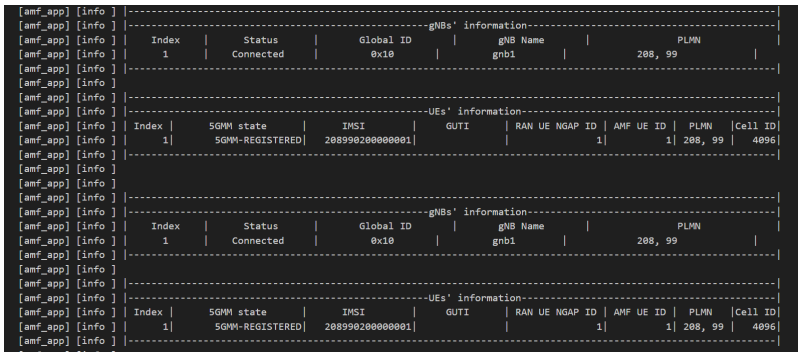

Figure 4.7: oai-amf log displaying both gNB and UE in connected state

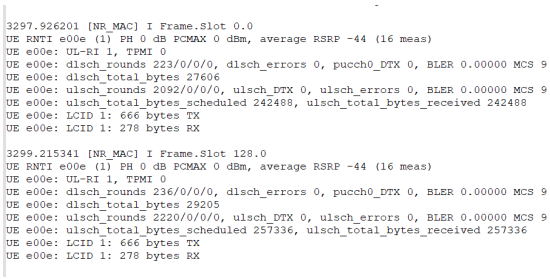

Figure 4.8: oai-gnb log displaying the connection and traffic exchanged between UE and gNB.

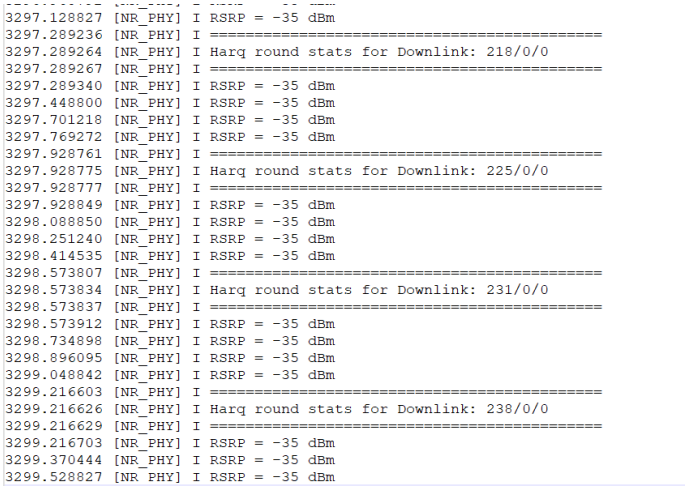

Figure 4.9: oai-nr-ue log displaying the connection and traffic exchanged between UE and gNB.

pair) during the simulations, as depicted in Figure 4.8. Additionally, the log captures any scheduling errors that occur as dlsch_errors for downlink and ulsch_errors for uplink.

In Figure 4.10, the data rate in uplink and downlink from gNB log can be seen. The gNB and UE start data transfer at around 3270 seconds in the simulation time upon establishing the PDU session. At the same time, the gNB sends a dedicated radio resource control (RRC) reconfiguration message to the UE, specifying the

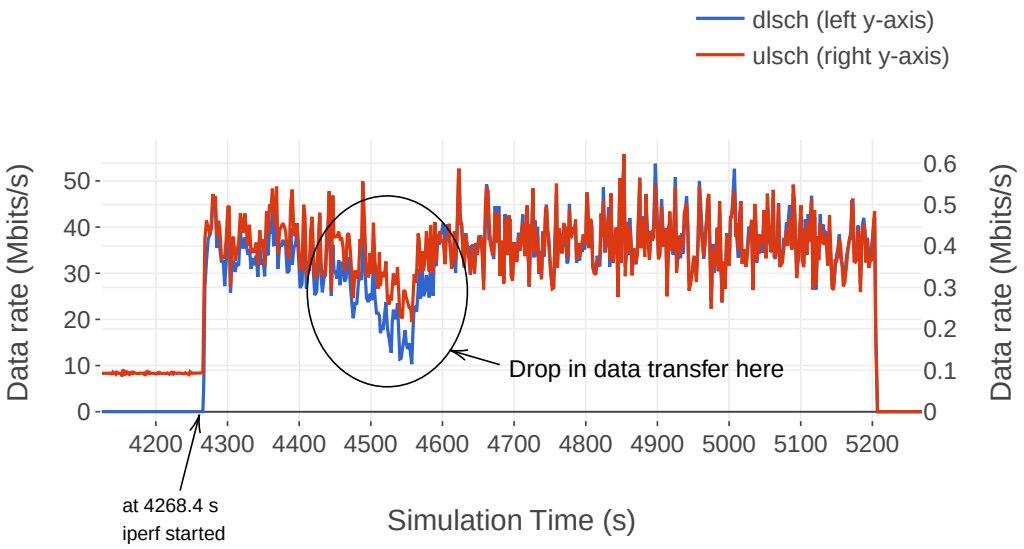

Figure 4.10: Plot illustrating the data bytes as observed in oai-gnb log.

configuration of the data radio bearer (DRB) that should be established at the UE to enable user plane traffic flow at the RAN stack. Data rate is observed at this time, with a downlink rate of approximately 0.01 Mbits/s. After these steps, the UE can exchange data through the CN. The iperf test began at simulation time 4268.4 s, as marked in Figure 4.10. The data rate increased significantly in response to the iperf reaching the range of 40 Mbits/s. While the reference signal received power (RSRP) at this point seems to have dropped, as shown in Figure 4.11, this is indicative of the cell edge condition seen in previous simulations which subsequently returns to the good signal range. The effect is due to the gNB scheduler adjusting the modulation and coding scheme (MCS) to compensate for the effects of signal quality based on the current channel conditions.

OAI supports link adaptation from which MCS is determined. Each MCS value represents the combination of modulation order and code rate. The scheduler chooses the MCS value in the range of 0 to 28. Initially MCS is guessed and is same for uplink and downlink. Based on the channel conditions and feedback from the UE, the performance of the link is dynamically adjusted by adjusting the MCS value. It also depends on the block error rate (BLER), which typically has a threshold of <10%. To maintain the BLER below this threshold in varying channel conditions, gNB adjusts the MCS accordingly as displayed in Figure 4.12 and Figure 4.13. The initial MCS index was 9 for both uplink and downlink. When iperf was started, the increased traffic load on the channels triggered gNB to adjust the downlink MCS to an appropriate value, as shown in Figure 4.12 so that it minimizes the BLER within the threshold. The link adaptation may have caused a drop in the data rate as seen in Figure 4.10 around 4500 to 4600 s, before it reached a more stable range until the UE is disconnected at 5200 s.

Before starting the scenario from the 3D simulator, each container is confirmed to be in healthy state. However, there is a simulation time mismatch between the logs

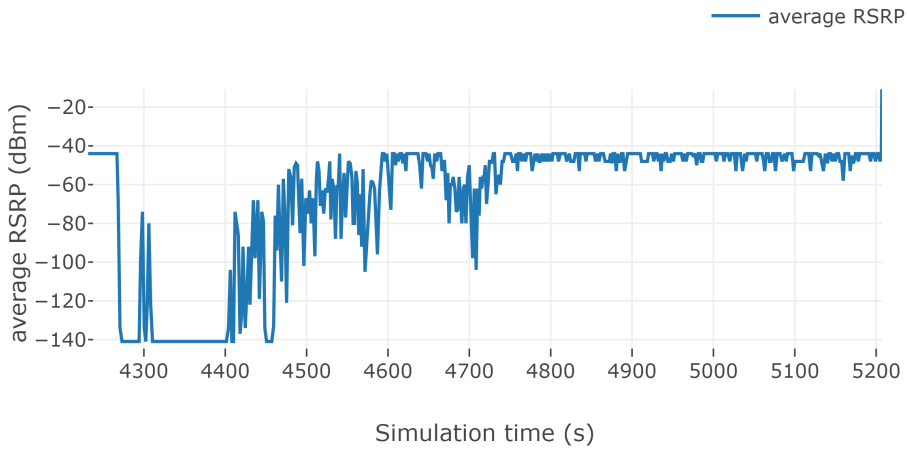

Figure 4.11: Plot illustrating the signal strength as RSRP as observed in oai-gnb log.

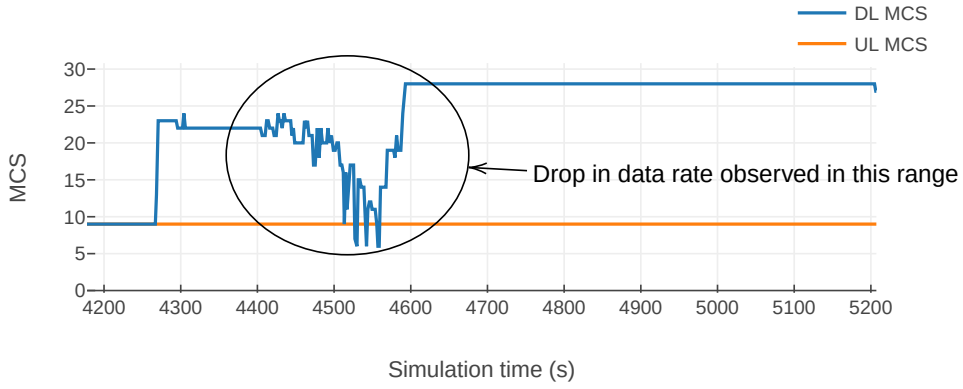

Figure 4.12: Plot illustrating the MCS adaptation as observed in oai-gnb log.

available in the OAI container and the 3D simulator. The OAI components do not always start logging from zero, while the simulation always logs from zero. This offset makes it difficult to align the data of OAI containers with the 3D simulator based on simulation time. In Figure 4.14, the path gain from the 3D simulator that runs in a separate container is shown. The simulation time stamps recorded in this log are different from other OAI containers. The path gain increases briefly just before the drop and was almost stable apart from these fluctuations. An interruption occurs around 2300 s, where the UE is disconnected as it moves behind the wall, as seen in previous simulations. Finding the offset might make it easier to observe the exact behaviour with respect to the UE movement that we see in the OAI container log. The disconnection is logged in the OAI logs as shown in Figure 4.15 and Figure 4.16.

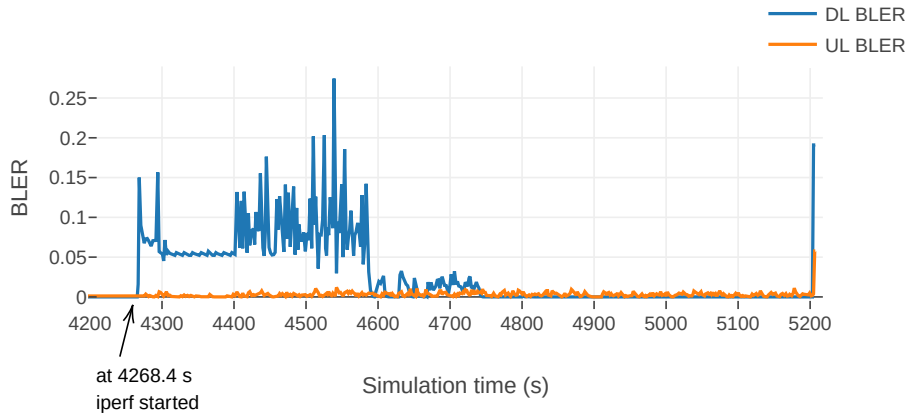

Figure 4.13: Plot illustrating the BLER as observed in oai-gnb log.

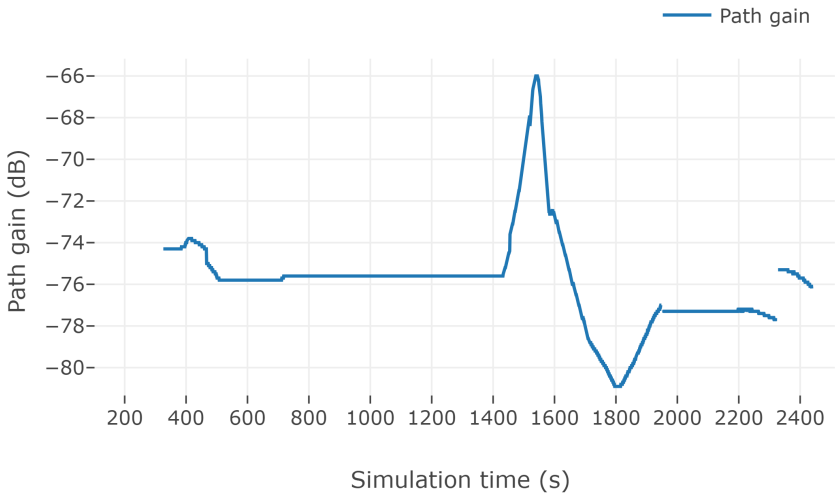

Figure 4.14: Plot illustrating the path gain as observed in tool log when connected to OAI.

The logs indicate that due to 'Error decoding PBCH' the UE declares a radio link failure and the oai-nr-ue container exits.

4.2.2 Ping and Iperf

When the gNB and UE are running and connected, their connectivity is tested by pinging oai-ext-dn (IP address 192.168.72.135) from the UE container oai-nr-ue1 through the tunnel interface *oaitun_ue*1 (IP address 12.1.1.2) assigned by 5G core network (5GCN). The ping statistics confirms a successful connection with the data packets received without any loss, as shown below:

```
5204.727265 [NR_MAC] I Frame.Slot 128.0
UE RNTI e00e (1) PH 0 dB PCMAX 0 dBm, average RSRP -48 (16 meas)
UE e00e: UL-RI 1, TPMI 0
UE e00e: dlsch_rounds 611271/15793/641/103, dlsch_errors 4, pucch0_DTX 0, BLER 0.00000 MCS 28
UE e00e: dlsch_total_bytes 4024576459
UE e00e: ulsch_rounds 378611/685/685/685, ulsch_DTX 0, ulsch_errors 685, BLER 0.00379 MCS 9
UE e00e: ulsch_total_bytes_scheduled 58466633, ulsch_total_bytes_received 58423905
UE e00e: LCID 1: 666 bytes TX
UE e00e: LCID 1: 278 bytes RX
UE e00e: LCID 4: 4000077478 bytes TX
UE e00e: LCID 4: 42531795 bytes RX

5205.735928 [NR_MAC] W Detected UL Failure on PUSCH after 10 PUSCH DTX, stopping scheduling
5205.736246 [NR_MAC] W Invalid timing advance offset for RNTI e00e
5205.737339 [NR_MAC] W Detected UL Failure on PUSCH after 11 PUSCH DTX, stopping scheduling
5206.382336 [NR_MAC] I Frame.Slot 256.0
UE RNTI e00e (1) PH 0 dB PCMAX 0 dBm, average RSRP -46 (8 meas)
UE e00e: UL-RI 1, TPMI 0
UE e00e: dlsch_rounds 611722/15892/664/122, dlsch_errors 16, pucch0_DTX 32, BLER 0.19099 MCS 27
UE e00e: dlsch_total_bytes 4028287844
UE e00e: ulsch_rounds 378832/694/690/689, ulsch_DTX 11, ulsch_errors 689, BLER 0.05772 MCS 9
UE e00e: ulsch_total_bytes_scheduled 58503138, ulsch_total_bytes_received 58460274
UE e00e: LCID 1: 666 bytes TX
UE e00e: LCID 1: 278 bytes RX
UE e00e: LCID 4: 4003770570 bytes TX
UE e00e: LCID 4: 42564860 bytes RX
```

Figure 4.15: oai-gnb log displaying the uplink failure message.

```
5207.146478 [NR_PHY] I ============================================
5207.146481 [NR_PHY] I Harq round stats for Downlink: 611718/15884/654/113
5207.146484 [NR_PHY] I ============================================
5207.146550 [NR_PHY] I RSRP = -83 dBm
5207.155466 [PHY] E [UE 0] frame 386, nr_slot_rx 0, Error decoding PBCH!
5207.165486 [PHY] E [UE 0] frame 388, nr_slot_rx 0, Error decoding PBCH!
5207.178221 [PHY] E [UE 0] frame 390, nr_slot_rx 0, Error decoding PBCH!
5207.187524 [PHY] E [UE 0] frame 392, nr_slot_rx 0, Error decoding PBCH!
5207.196782 [PHY] E [UE 0] frame 394, nr_slot_rx 0, Error decoding PBCH!
5207.206139 [PHY] E [UE 0] frame 396, nr_slot_rx 0, Error decoding PBCH!
5207.215296 [PHY] E [UE 0] frame 398, nr_slot_rx 0, Error decoding PBCH!

Assertion (0) failed!
In nr_rrc_handle_timers() ../../../openair2/RRC/NR_UE/rrc_timers_and_constants.c:120
Radio link failure! Not handled yet!
5207.233121 [PHY] E [UE 0] frame 400, nr_slot_rx 0, Error decoding PBCH!
5207.233206 [NR_PHY] I RSRP = -81 dBm
5207.250951 [PHY] E [UE 0] frame 402, nr_slot_rx 0, Error decoding PBCH!
5207.259559 [PHY] E [UE 0] frame 404, nr_slot_rx 0, Error decoding PBCH!
5207.265631 [NR_MAC] I [UE 0] Release all SRs
5207.267011 [PHY] E [UE 0] frame 406, nr_slot_rx 0, Error decoding PBCH!
5207.274268 [PHY] E [UE 0] frame 408, nr_slot_rx 0, Error decoding PBCH!
```

Figure 4.16: oai-nr-ue log displaying the radio link failure message.

```
$ ping 192.168.72.135 -c 10
PING 192.168.72.135 (192.168.72.135) 56(84) bytes of data.
64 bytes from 192.168.72.135: icmp_seq=1 ttl=64 time=0.100 ms
64 bytes from 192.168.72.135: icmp_seq=2 ttl=64 time=0.041 ms
64 bytes from 192.168.72.135: icmp_seq=3 ttl=64 time=0.055 ms
64 bytes from 192.168.72.135: icmp_seq=4 ttl=64 time=0.051 ms
64 bytes from 192.168.72.135: icmp_seq=5 ttl=64 time=0.057 ms
64 bytes from 192.168.72.135: icmp_seq=6 ttl=64 time=0.054 ms
64 bytes from 192.168.72.135: icmp_seq=7 ttl=64 time=0.053 ms
64 bytes from 192.168.72.135: icmp_seq=8 ttl=64 time=0.054 ms
64 bytes from 192.168.72.135: icmp_seq=9 ttl=64 time=0.050 ms
64 bytes from 192.168.72.135: icmp_seq=10 ttl=64 time=0.066 ms

--- 192.168.72.135 ping statistics ---
10 packets transmitted, 10 received, 0% packet loss, time 9209ms
rtt min/avg/max/mdev = 0.041/0.058/0.100/0.015 ms
```

The measured round trip time (RTT) in the ping test above appears to be lower than expected. No packet loss has been detected, confirming a successful connection. Although it is possible that the ping test was not routed in the same way as the

iperf test. However, it was not possible to repeat the test to confirm this and it was not explored.
The data traffic between the UE (oai-nr-ue1) and external data network (oai-ext-dn) is tested using iperf3 through the following command on server (oai-ext-dn) node with TCP connection:

```
$ docker exec -it oai-ext-dn iperf3 -s
```

In another terminal, the iperf3 is started on the client (oai-nr-ue1) node:

```
$ docker exec -it oai-nr-ue1 iperf3 -B 12.1.1.2 -c 192.168.72.135
```

The commands above would perform an uplink data connection test where the client sends and the server receives. By adding the -R option at the client side, the sender can be reversed, resulting in a downlink connection.

Figure 4.17: Iperf3 test showing the established connection between UE and gNB

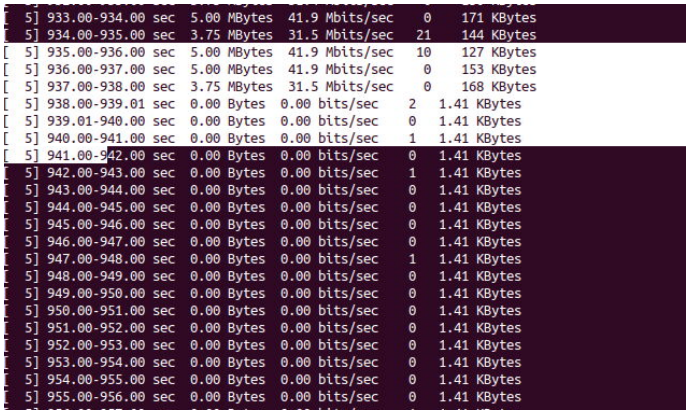

Figure 4.18: Iperf3 test snippet of server node demonstrating the termination of a connection when the UE moves out of coverage and does not re-establish connection with gNB.

By default, the iperf test will run for 10 seconds, this is increased to 1000 seconds to observe the changes in traffic patterns with mobility in the UE. The Figure 4.17 illustrates the establishment of a downlink connection between two nodes with data transfer between them as confirmed by the iperf test. However, if the UE experiences signal loss, as seen in previous tool simulations, this is also reflected in this test.

When the connection is terminated, the UE does not re-establish the connection to the gNB as shown in Figure 4.18. This indicates that the configuration is working correctly, although it appears to be affected by the reception.
The Figure 4.19 illustrates the data rate observed in oai-gnb log as a logical channel data transfer when the iperf test is performed. It follows the same pattern as the rest of the observations and ultimately the UE becomes disconnected. Both Figure 4.18 and Figure 4.19 indicate that UE got disconnected approximately around 936 s of simulation time. A data rate of 33 Mbits/s on average was observed on the DL from the iperf measurement.

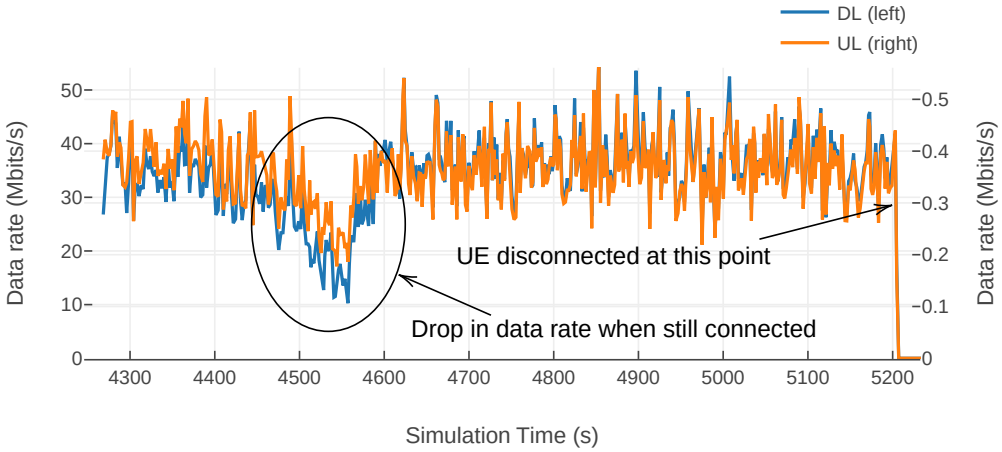

Figure 4.19: Plot illustrating the iperf data rate as observed from oai-gnb log.

The scenario connected from the tool did not load the multipath propagation, which may have caused the UE to disconnect. However, as previously seen, the UE will regain coverage and could reconnect. As observed from oai-gnb and oai-nr-ue logs, the UE failed to re-establish the connection. This behaviour highlights a limitation of OAI, particularly in scenarios involving mobility. The issues in simulating seamless handovers and re-connections highlight an area for potential improvement in the capabilities of OAI, especially in dynamic scenarios with mobile users.

4.3 Comparison of Simulation Results with Theoretical Model

In this section the metrics calculated from the theoretical benchmark are compared with the values obtained from the simulation logs of the tool. Apart from a direct comparison with the values from tool, the effect of transmit power, carrier frequency and bandwidth on the performance of the link is investigated. The parameter and their values considered for simulation are listed in Table 4.1.

Table 4.1: Simulation parameters for theoretical benchmark

Parameter	Value
Carrier frequency (f_c)	4 GHz
Bandwidth (BW)	20 MHz
Antenna Gain - Transmitter and receiver (G)	0 dB
Noise figure (NF)	6 dB
BS antenna height	3 m
UE antenna height	1 m

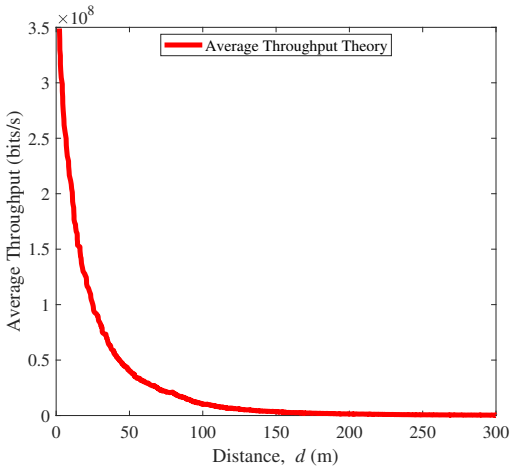

Figure 4.20: Convergence of throughput over distance.

In Figure 4.20, the performance of the system model is shown for the channel model discussed in Section 2.3.1 and the parameters described in Table 4.1. The graph depicts the relationship between average throughput and distance between BS and UE. Based on 1000 iterations, the average throughput tends to zero at a distance of 200 m. This convergence is crucial to validate the accuracy of the channel model. The decreasing throughput highlights the effect of increasing distance on SNR. As the distance increases, the received signal weakens, leading to greater path loss and a subsequent reduction in SNR, causing a gradual decrease in throughput. In the following sections, the performance of the system is evaluated for various parameters.

4.3.1 Received Power and Throughput

The received power from the theoretical model over the range of distance mentioned for an indoor scenario is illustrated in Figure 4.21.

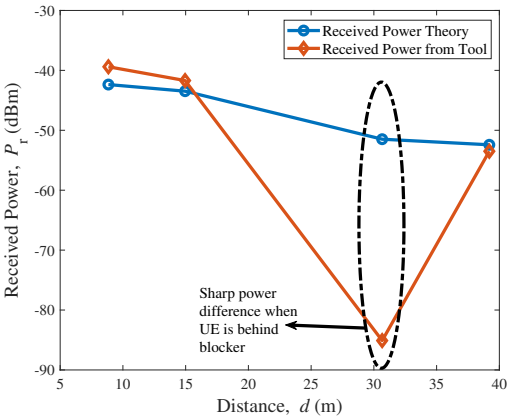

Figure 4.21: Comparison of Received Power: Theoretical Model and DT Tool over distances

The figure presents two measurements of received power; one depicts the power obtained directly from the tool, whereas the curve in blue shows the power determined based on the distances calculated from the UE's position in the tool. It is evident that the power extracted directly from the tool exhibits sharp fluctuations at points when the UE is obstructed. This particular blockage phenomenon is more accurately depicted in the tool than in the theoretical values. The blockage in theory is based on the LOS probability as in (2.3), which is inherent in the model used. According to the LOS probability, at $d = 30.66$ m, the path will be considered as LOS, however in reality there is a blocker, which explains the difference in the values of P_r. Even though, both models have blockage, because of the dependency over distance, it is not being reflected in theory as it does with the tool.

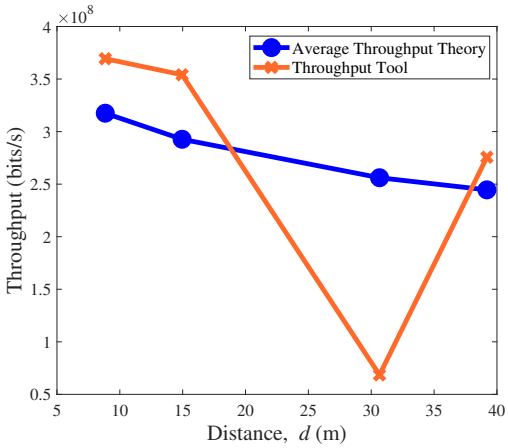

Figure 4.22: Comparison of Throughput: Theoretical Model and DT Tool over varying distances

In Figure 4.22 the average throughput over a number of iterations in the theory is shown alongside the one calculated from the received power from the tool. Here, the throughput from the tool is calculated based on the received power and is not an average over many iterations.

4.3.2 Effect of Transmit Power

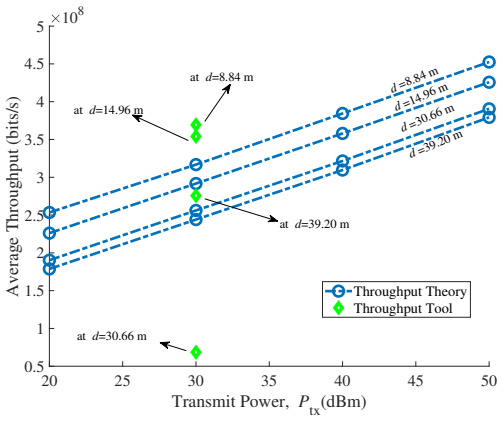

Figure 4.23: The effect of varying P_{tx} on theoretical average throughput at selected distances

Figure 4.23 illustrates the average throughput obtained over 1000 iterations as a function of transmit power levels at selected distances between BS and UE. This allows an estimate of what could be achieved by the changes in transmit power, assuming all other parameters remain the same. A significant trend shows that for shorter distance at $d = 8.84$ m, the throughput at the same level of P_{tx} exceeds that is observed at longer distances. This indicates the limitations associated with signal propagation over increasing distances, where path loss and multipath fading reduce the SNR. As a result, the system is more sensitive to changes in transmit power at greater distances, leading to a noticeable decrease in throughput as expected. Additionally, it is also noted that an increase in P_{tx} is consistently associated with an improvement in throughput, regardless of distance. This highlights the critical impact of transmit power in compensating for distance-related losses, resulting in improved system performance. The intention of the demonstrations were to identify the use cases, synergies and differences in predictions for the tool and theoretical model without the loss of generality. However, more in detailed analysis on the theoretical modelling and performances can be performed, although is not the focus of this work.

4.3.3 Effect of Carrier Frequency and Bandwidth

The Figure 4.24 illustrates the average throughput as a function of f_c and BW at selected distances between the BS and the UE. In this case, the frequency range up to 5 GHz has been considered. It is observed that the BW has a significant effect on the throughput at the same f_c. An increase in bandwidth and minimum distance results in a significant increase in throughput at the same frequency. Similarly, as the f_c increases, the throughput tends to decrease. Therefore, as the f_c is increased, if the BW is not adjusted accordingly, there is a possibility that the throughput will be reduced. The graph shows that an optimal combination of f_c and BW exists for certain distances, which maximizes throughput. The simulations in the tool are

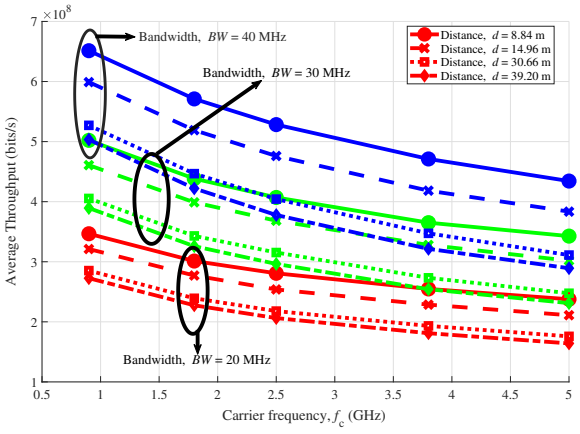

Figure 4.24: The effect of f_c and BW on theoretical average throughput up to 5 GHz at selected distances

performed with $BW = 20$ MHz and $f_c = 4$ GHz and at the same distances as those used in the graph.

5
Conclusion

This thesis work explored the concept of the network digital twin (NDT) by successfully running 3D simulations in the tool, testing multiple scenarios and analysing the results. The study focused on 5G network simulations using advanced tools and methods to instigate insights on the digital twin (DT). The study aimed to integrate the 3D simulation tool with the OpenAirInterface (OAI) software stack to create an end-to-end network simulator that depicts the network digital twin (NDT). The methods comprised three parts. The first involved performing simulations solely with the 3D simulation tool. The second involved integrating the tool with OAI, while the final part compared the results of the first part with a standard theoretical model. Various simulations were conducted to examine network performance under different scenarios. The simulations performed allowed for the collection and analysis of valuable data, shedding light on the behavior of the DT. This chapter presents a summary of the main findings and discusses their implications in the dynamic field of 5G network simulation and analysis.

In the 3D simulations using the tool, it demonstrated better performance compared to the theoretical model. The simulations using OAI aim to explore the integration of baseband and core network functionality into simulations. This integration is motivated by the current absence of data plane functionality in the tool, making the implementation of OAI a first step towards a more comprehensive simulation environment. It is important to note that the minimalist deployment version of OAI has been used for this integration, providing a basic context for exploring the implemented features. However, it is essential to acknowledge certain limitations, specifically to the current implementation context, such as the fact that UE does not re-establish a connection when a connection has been lost. In a typical cellular network, when a UE moves out of coverage and then returns within range, it should attempt to re-establish a connection with the gNB, a process known as cell reselection. However, in this experiment, the UE did not re-establish the connection. Of course, the results will be affected by the OAI deployment in terms of network configuration, resources available for the docker services to run and specific parameters choices. Addressing this can significantly improve reliability and performance.

There are some observations such as the measurement logs from the tool simulations for a user moving around the room in the scenario lack information on the exact position of the user. Therefore, manual pinpointing was used to locate the user position. This might have caused the steep drop in the measured values where a smoother transition would have been more appropriate. The theoretical blockage model has limitations in objectively explaining obstacle complexity, as it heavily relies on the distance between the UE and BS. This is evident in the differences

observed in the comparison. In contrast, the DT model excels in accurately locating blockers, showcasing promise for enhanced precision. The deviations are attributed to differences in antenna configurations, transmitter and receiver positions, and several other factors. The reliability of the throughput obtained from the OAI Iperf test is limited because it is not exactly synchronised with the movement of the UE. Although the current study focused on the indoor scenario, the findings provide a starting point for exploring combinations of additional scenarios and parameters.

6
Future Work

There are opportunities to extend the scope and capabilities of current work. One approach is to use machine learning and automation techniques to extract insights from simulation data for effective analysis of logs, enabling predictions of failures and other outcomes. Another important aspect is to conduct simulations in diverse scenarios with OAI to understand their usability in these cases. Using real network data or a more robust theoretical model with additional input parameters would provide a better comparison. Another aspect would be to investigate the scalability of the network by introducing several gNBs and UEs with OAI. This would provide valuable insights into the performance of the tool in a multi-user environment. Realtime, scalable and fast RF mapping of actual environments using the capabilities of machine learning techniques and higher GPU powers is an important direction to explore. Moreover, the digital twin model is an evolving representation and requires continuous improvement to address discrepancies between digital and real environments. Addressing the challenges of capturing complex details and moving objects efficiently would pave the way for more accurate and realistic digital representations in future endeavours.

Bibliography

[1] M. Shafi, A. F. Molisch, P. J. Smith, *et al.*, "5G: A Tutorial Overview of Standards, Trials, Challenges, Deployment, and Practice," *IEEE Journal on Selected Areas in Communications*, vol. 35, no. 6, pp. 1201–1221, 2017. DOI: 10.1109/JSAC.2017.2692307.

[2] Ericsson blog, *Next-generation simulation technology to accelerate the 5G journey.* [Online]. Available: https://www.ericsson.com/en/blog/2021/4/5g-simulation-omniverse-platform.

[3] Ericsson Technology Review article, "Realizing 5G smart-port use cases with a digital twin," [Online]. Available: https://www.ericsson.com/en/reports-and-papers/ericsson-technology-review/articles/realizing-5g-smart-port-use-cases-with-a-digital-twin.

[4] B. R. Barricelli, E. Casiraghi, and D. Fogli, "A Survey on Digital Twin: Definitions, Characteristics, Applications, and Design Implications," *IEEE Access*, vol. 7, pp. 167 653–167 671, 2019. DOI: 10.1109/ACCESS.2019.2953499.

[5] D. J. Wagg, K. Worden, R. J. Barthorpe, and P. Gardner, "Digital Twins: State-of-the-Art and Future Directions for Modeling and Simulation in Engineering Dynamics Applications," vol. 6, no. 3, May 2020, ISSN: 2332-9017. DOI: 10.1115/1.4046739.

[6] A. Fuller, Z. Fan, C. Day, and C. Barlow, "Digital Twin: Enabling Technologies, Challenges and Open Research," *IEEE Access*, vol. 8, pp. 108 952–108 971, 2020. DOI: 10.1109/ACCESS.2020.2998358.

[7] Ericsson Technology Review article, "Network digital twins - outlook and opportunities," [Online]. Available: https://www.ericsson.com/en/reports-and-papers/ericsson-technology-review/articles/network-digital-twins-outlook-and-opportunities?video-dialog=1_tqlso3wq.

[8] F. Tao, M. Zhang, and A. Nee, *Chapter 2 - Applications of Digital Twin*, F. Tao, M. Zhang, and A. Nee, Eds. Academic Press, 2019, pp. 29–62, ISBN: 978-0-12-817630-6. DOI: https://doi.org/10.1016/B978-0-12-817630-6.00002-3. [Online]. Available: https://www.sciencedirect.com/science/article/pii/B9780128176306000023.

[9] [Online]. Available: https://www.ericsson.com/en/network-services/deployment/site-digital-twin.

[10] M. M. Zoltick and J. B. Maisel, "Societal impacts: Legal, regulatory and ethical considerations for the digital twin," in *The Digital Twin*, N. Crespi, A. T. Drobot, and R. Minerva, Eds. Cham: Springer International Publishing, 2023, pp. 1167–1200, ISBN: 978-3-031-21343-4. DOI: 10.1007/978-3-031-21343-4_37.

[11] M. Grieves, "Digital Twin: Manufacturing Excellence through Virtual Factory Replication," Mar. 2015. [Online]. Available: https://www.researchgate.net/publication/275211047_Digital_Twin_Manufacturing_Excellence_through_Virtual_Factory_Replication.
[12] M. Grieves, "Don't 'twin' digital twins and simulations opinion," Dec. 2022. [Online]. Available: https://www.researchgate.net/publication/365991616_Don%27t_%27Twin%27_Digital_Twins_and_Simulations_Opinion.
[13] [Online]. Available: https://www.nsnam.org/.
[14] [Online]. Available: https://www.amarisoft.com/.
[15] [Online]. Available: https://omnetpp.org/.
[16] [Online]. Available: https://se.mathworks.com/help/comm/ref/wirelessnetworksimulator.html.
[17] [Online]. Available: https://opnetprojects.com/opnet-network-simulator/.
[18] [Online]. Available: https://openairinterface.org/.
[19] [Online]. Available: https://www.3gpp.org/about-3gpp.
[20] *4g/5g software*. [Online]. Available: https://www.northeastern.edu/colosseum/cellular-software/.
[21] 3GPP TR 38.901 v17.0.0, "Study on Channel Model for Frequencies from 0.5 to 100 GHz (Release 17)," [Online]. Available: https://www.3gpp.org/ftp/Specs/archive/38_series/38.901/ (visited on 03/31/2023).
[22] [Online]. Available: https://www.blender.org/.
[23] [Online]. Available: https://openairinterface.org/oai-5g-core-network-project/.
[24] *5G;NR; Requirements for support of radio resource management (3GPP TS 38.133 version 17.11.0 Release 17)*, 2023. [Online]. Available: https://www.etsi.org/deliver/etsi_ts/138100_138199/138133/17.11.00_60/ts_138133v171100p.pdf.
[25] *OpenAirInterface 5G-OTA*, 2023. [Online]. Available: https://gitlab.flux.utah.edu/powderrenewpublic/mww2023/-/blob/main/content/oai_ota.md.

DEPARTMENT OF ELECTRICAL ENGINEERING
CHALMERS UNIVERSITY OF TECHNOLOGY
Gothenburg, Sweden 2024
www.chalmers.se

CHALMERS
UNIVERSITY OF TECHNOLOGY